A Novel Communication System of High Capacity

Michel Fattouche

***Abstract*—An objective of this article is to design a novel communication system that is capable of offering substantial improvement in channel capacity compared to band-limited (BL) communication systems, when constrained by the same spectral mask. To this end, this article has two contributions. The first contribution is theoretical. It derives the capacity of a time-limited (TL) system across a mask-constrained channel contaminated by interference and by additive white Gaussian noise, where doubling the channel capacity requires only a *fixed* multiple increase in average received signal-to-noise ratio (SNR). This is in contrast with BL systems, which require a *geometric* multiple increase in SNR. The second contribution is practical. It takes advantage of the theory established in the first objective to design a novel TL system. This article shows several designs of the novel system for a centralized multiple access (MA) wireless network, which outperform current MA networks by an order of magnitude, including one design that is shown to meet future 5G specifications without requiring mm-wave bands.**

***Index Terms*—Fifth generation (5G) without mm-wave bands, degrees of freedom, finite access time, mask matched, time limited (TL).**

I. Introduction

FIFTH-GENERATION (5G) wireless systems promise to deliver $\geq$10 Gb/s download capacity across mm-wave bands (26, 28, 38, and 60 GHz) with an estimated median bandwidth (BW) of 3.5 GHz. Such bands suffer from a high path loss (PL) and are not multipath rich. The high PL restricts coverage to line-of-sight (LOS) communication, whereas a poor multipath environment limits the number of spatial degrees of freedom (DOF) in a multiple-input–multiple-output (MIMO) system. By taking advantage of the existence of high-frequency components in a time-limited (TL) system, this article shows how to meet the 10 Gb/s requirement for 5G systems without requiring mm-wave bands.

Wyner [1] first studied the capacity of a TL system in 1966, after constraining it to be *approximately* band limited (BL). When the system is instead constrained to be *root-mean-square* (rms) BL, reducing interference between input signals is accomplished by minimizing the rms BW of each signal. The solution of such a minimization was shown by Gabor in [2] to be one lobe of a sine wave, a solution used subsequently in numerous papers [3]–[5].

Over time, the notion that practical communication systems are *approximately* BL was replaced by the notion that they are indeed BL [6], [7] as far as the channel capacity is concerned. This was because it was thought [8] that the high-frequency components, which exist in a TL system and which fall far below the noise floor when the system is constrained by a spectral mask, could not realistically contribute to the channel capacity of the TL system. This article shows that such components can indeed contribute significantly to the channel capacity based on the fact that they represent an arbitrarily large number of DOF with the ability to offer a linear signal-to-noise ratio (SNR) contribution toward the capacity. This is in contrast with BL systems where all DOF can only offer a logarithmic SNR contribution toward the capacity. The notion that TL systems are able to offer an arbitrarily large number of DOF was also observed in [3] and [9], however, without realizing their ability to offer a linear SNR contribution toward the capacity.

By taking advantage of such ability, it is possible to force the channel capacity of the TL system to contain a new SNR region, referred to as the *medium* SNR region, in addition to the traditional *low*- and *high*-SNR regions found in the capacity of a BL system [6]. The newly created SNR region allows for the design of a novel TL system where doubling channel capacity requires only a fixed multiple increase in SNR, as opposed to a BL system, which requires a geometric multiple increase [8]. The novel TL system loads $\approx$1 b of information per complex DOF. This is in contrast [6, p. 164] with either the low-SNR region, which loads $<$1 b of information per complex DOF, or the high-SNR region, which typically loads $>$1 b of information per complex DOF.

Recently, several systems found a way to increase the number of their DOF. Such systems include multiuser systems [7], [10], [11], which form the basis for 3G wireless systems, and MIMO systems [12]–[14], which are currently adopted in most cellular standards, including 4G and 5G wireless systems. Multiuser systems correspond to having K colocated users, each with a spreading gain N, which is the number of their DOF, whereas MIMO systems correspond to having K transmit antennas and N receive antennas where the number of DOF $\leq \min\{K, N\}$ [13]. Despite the fact that both systems have the ability to arbitrarily increase the number of their DOF, their respective capacities do not contain a medium SNR region since both systems fail to realize that, under certain conditions, some DOF can offer a linear SNR contribution toward the capacity.

This article is structured as follows. Section II presents Theorems I, II, and III, which derive the capacity of a TL system across a communication channel contaminated by additive white Gaussian noise (AWGN) and by interference, with and without a mask constraint. Section III introduces three steps for designing a novel TL system, based on Theorems I and III and also on achieving a desired capacity $\mathcal{C}_\mathfrak{d}$. The first design step selects the number of DOF required for achieving $\mathcal{C}_\mathfrak{d}$. The second design step enhances the contribution of the selected DOF, whereas the third design step randomizes the DOF using a pseudo-random (PR) phase. Theorem IV generalizes Theorem III by including the effects of the selected, enhanced, and randomized DOF in the novel TL system across an interference-limited mask-constrained channel. Section IV proposes a system

Manuscript received June 7, 2019; revised September 2, 2019 and December 9, 2019; accepted December 12, 2019. Date of publication January 13, 2020; date of current version September 2, 2020.

The author is with the Department of Electrical and Computer Engineering, The University of Calgary, Calgary, AB T2N 1N4, Canada (e-mail: mtfattou@ucalgary.ca).

Digital Object Identifier 10.1109/JSYST.2019.2961131

architecture that is adequate for the novel TL system. Section V implements three designs of the novel TL system, which outperform current centralized mask-constrained MA networks by an order of magnitude, with Section VI compiling the results of their downlink and uplink portions. Section VII concludes this article.

II. TL Systems

Based on the multiuser model in [7, eq. (1.1)], an information vector $\vec{\alpha} \in \mathbb{C}^{Q\times 1}$, consisting of Q information symbols, can be transmitted as a vector $\vec{x} \in \mathbb{C}^{M\times 1}$, defined as

$$\vec{x} \triangleq \boldsymbol{h}\vec{\alpha}. \tag{1}$$

Unlike $\boldsymbol{h}$ in [7], which is an $N \times K$ block matrix, $\boldsymbol{h} \in \mathbb{C}^{M\times Q}$ in (1) is a block Toeplitz [15] matrix. In other words

$$\boldsymbol{h} \triangleq \mathrm{toep}_{\mathcal{d}}\{\vec{\boldsymbol{h}}\} \tag{2}$$

where $\mathrm{toep}_{\mathcal{d}}\{\vec{\boldsymbol{h}}\}$ is an operator, which forms $\boldsymbol{h}$ by repeatedly replicating the submatrix $\vec{\boldsymbol{h}}$ to the right $L-1$ times, while cyclically shifting $\vec{\boldsymbol{h}}$ down by $\mathcal{d}$ rows for every single replica to the right, with L defined as, the ceiling of Q/K. $\vec{\boldsymbol{h}} \in \mathbb{C}^{M\times K}$ is defined as $\vec{\boldsymbol{h}} \triangleq [\begin{smallmatrix}\boldsymbol{h}_{\mathrm{Basic}}\\ \mathbf{0}_{\mathcal{d}(L-1)\times K}\end{smallmatrix}]$ where $\boldsymbol{h}_{\mathrm{Basic}} \in \mathbb{C}^{N\times K}$ is referred to as the *basic building block*, whereas $\mathbf{0}_{\mathcal{d}(L-1)\times K}$ is the all zero matrix, with $\mathcal{d} \leq N$ and $M \triangleq N + \mathcal{d}(L-1)$.

Interpretation of $\boldsymbol{h}$: Since each column of $\boldsymbol{h}$ is responsible for transporting one information symbol in $\vec{\alpha}$, therefore, $\vec{x}$ in (1) can model a $K-$user TL system with *spreading gain* [7] $N < \infty$ with a number $K_{\mathfrak{d}}$ of *desired* transmitters (Txs) intended for a receiver Rx and a number $K_{\mathfrak{i}}$ of *interfering* Txs, s.t. $K = K_{\mathfrak{d}} + K_{\mathfrak{i}}$. We assume in this article that $K_{\mathfrak{d}} = 1$ and that the kth active Tx transmits a vector $\vec{x}_k$ transporting the set of L symbols, $\{\alpha_k, \alpha_{k+K}, \ldots, \alpha_{k+(L-1)K}\}$, after converting $\vec{x}_k$ into a continuous-time signal, $x_k(t)$, of finite duration MT_s, with T_s the duration of one sample in $\vec{x}$.

Theorem I assumes the following.

1) The kth Tx transmits $x_k(t)$ subject to Constraint 1

$$\text{Constraint 1: } \int_{-\infty}^{\infty} \mathcal{S}_{x_k(t)}(f)\, df \leq \mathfrak{p} \quad \forall k$$

where $\mathfrak{p}$ is the average allocatable transmit power at any Tx.

2) The kth Tx transmits $x_k(t)$ using a single antenna across a communication channel where it is received at Rx using a single antenna. The received signal $y(t)$ is then sampled at Rx at a sampling frequency $f_s \triangleq 1/T_s$ to form a discrete-time signal $\vec{y} \in \mathbb{C}^{\mathcal{M}\times 1}$ defined as

$$\vec{y} \triangleq \boldsymbol{h}_{\mathrm{Ch}}\, \vec{\alpha} + \vec{w} \tag{3}$$

where $\boldsymbol{h}_{\mathrm{Ch}} \in \mathbb{C}^{\mathcal{M}\times Q}$ corresponds to $\boldsymbol{h}$ after including the effects of the channel, such as replacing M by a number $\mathcal{M} \geq M$, and $\vec{w} \in \mathbb{C}^{\mathcal{M}\times 1}$ models the WGN. We refer to the combination of the TL system and channel as a TL *channel*.

Theorem I: The capacity $\mathcal{C}_{\mathrm{TL}}$ of the TL channel corresponding to $\boldsymbol{h}_{\mathrm{Ch}}$ in (3), subject to Constraint 1, is

$$\mathcal{C}_{\mathrm{TL}} = \frac{1}{MT_s} \sum_{k=1}^{\mathrm{rank}(\boldsymbol{h}_{\mathrm{Ch}})} \log_2\left(1 + \Lambda_k \frac{\bar{\mathcal{A}}K\mathfrak{p}}{\mathbb{N}_o f_s}\right) \text{b/s} \tag{4}$$

where $\mathbb{N}_o/2$ is the two-sided power spectral density (PSD) of the WGN, $\bar{\mathcal{A}}$ is the average attenuation in power across the channel, and Λ_k is the kth-squared singular value of a normalized $\boldsymbol{h}_{\mathrm{Ch}}$ s.t. its kth column $\{\boldsymbol{h}_{\mathrm{Ch}}\}_k$ has on average an L2-norm, which equals $\mathcal{d}$ $\forall k$.

Proof of Theorem I: See Appendix A.

Importance of Theorem I: $\mathcal{C}_{\mathrm{TL}}$ in (4) consists of several regions, which depend on the average received TL SNR, $\frac{\bar{\mathcal{A}}K\mathfrak{p}}{\mathbb{N}_o f_s}$. Similar to the capacity $\mathcal{C}_{\mathrm{BL}}$ of a BL system [10], $\mathcal{C}_{\mathrm{TL}}$ in (4) consists of a low-SNR region and a high-SNR region. Unlike BL systems, $\mathcal{C}_{\mathrm{TL}}$ in (4) also contains a new *medium*-SNR region, when a number $\mathfrak{n}$ of the terms $\Lambda_k \frac{\bar{\mathcal{A}}K\mathfrak{p}}{\mathbb{N}_o f_s}$ in (4) are $\ll 1$ s.t. $\log_2(1 + \Lambda_k \frac{\bar{\mathcal{A}}K\mathfrak{p}}{\mathbb{N}_o f_s}) \approx \log_2 e\ \Lambda_k \frac{\bar{\mathcal{A}}K\mathfrak{p}}{\mathbb{N}_o f_s}$. When $\mathcal{C}_{\mathrm{TL}}$ is in the low-SNR region, $\mathfrak{n} = \mathrm{rank}(\boldsymbol{h}_{\mathrm{Ch}})$. When $\mathcal{C}_{\mathrm{TL}}$ is in the high-SNR region, $\mathfrak{n} = 0$. When $\mathcal{C}_{\mathrm{TL}}$ is in the medium-SNR region, $0 < \mathfrak{n} \leq \mathrm{rank}(\boldsymbol{h}_{\mathrm{Ch}})$.

Given that the communication channel in this article is to be constrained by a spectral mask, Theorem I must be modified to include a mask constraint. First, we define the BW of $x_k(t)$; then, we introduce the mask constraint.

Definition of the BW of $x_k(t)$: Since $x_k(t)$ is TL, its PSD $\mathcal{S}_{x_k(t)}(f)$ exists over the entire frequency domain $f \in \{-\infty, \infty\}$, allowing for numerous definitions of BW to exist. In this article, we adopt the same definition of BW as the one adopted by the International Telecommunication Union (ITU) [16], which defines transmitter spectrum emissions as falling into three distinct bands: 1) *occupied band emission* with a BW $\mathcal{W}$; 2) *out-of-band-emission* (OOBE) band with a BW $\mathcal{W}_{\mathrm{OOBE}}$; and (c) *far-out-spurious-emission* (FOSE) band with an allowable power level $\leq \frac{1}{\mathcal{R}}$. By adopting the same definition for BW as the ITU, we select the BW $\mathcal{W}_{\mathrm{TL}}$ of the TL system to be defined as the BW $\mathcal{W}$ of the occupied band.

Spectral Mask Constraint: All systems considered in this article are constrained by a spectral mask $\mathbb{P}_{\mathrm{Mask}}(f)$. In other words, $x_k(t)$ is subject to Constraint 2

$$\text{Constraint 2: } \mathcal{S}_{x_k(t)}(f) \leq \beth \mathbb{P}_{\mathrm{Mask}}(f) \quad \forall f, \forall k$$

where $\beth$ is a normalization constant, which depends on $\mathfrak{p}$, $\mathbb{P}_{\mathrm{Mask}}(f)$, and $\boldsymbol{h}$. According to the ITU, $\mathcal{W}$ must be selected $\leq \mathcal{W}_m$ where $\mathcal{W}_m$ is the BW of $\mathbb{P}_{\mathrm{Mask}}(f)$. This implies that $\mathcal{W}_{\mathrm{TL}}$ must be selected $\leq \mathcal{W}_m$ as well. For this reason, we define in this article an *overhead factor*, $\boldsymbol{\mathcal{r}} \triangleq \mathcal{W}_{\mathrm{TL}} N T_s \geq 1$, as the overhead, both in time and in frequency, which is required for $x_k(t)$ to comply with Constraint 2. It is selected such that $\mathcal{W}_{\mathrm{TL}} \leq \mathcal{W}_m$ or equivalently, N is selected s.t. $N \geq N_{\min} \triangleq \frac{\boldsymbol{\mathcal{r}}}{\mathcal{W}_m T_s}$.

Under Constraints 1 and 2, $\mathcal{C}_{\mathrm{TL}}$ in (4) can be expressed as

$$\mathcal{C}_{\mathrm{TL}} = \frac{\mathcal{W}_m}{\boldsymbol{\mathcal{r}}} \frac{N_{\min}}{M} \sum_{k=1}^{\mathrm{rank}(\boldsymbol{h}_{\mathrm{Ch}})} \log_2\left(1 + \frac{\Lambda_k \boldsymbol{\mathcal{r}}}{N_{\min}} \frac{\bar{\mathcal{A}}K\mathfrak{p}}{\mathbb{N}_o \mathcal{W}_m}\right). \tag{5}$$

Similarly, under Constraints 1 and 2, a BL system, of fixed BW $\mathcal{W}_{\mathrm{BL}}$ selected as $\mathcal{W}_{\mathrm{BL}} = \mathcal{W}_m$ has a BL capacity $\mathcal{C}_{\mathrm{BL}}$ given as [10]

$$\mathcal{C}_{\mathrm{BL}} = \frac{\mathcal{W}_m}{\boldsymbol{\mathcal{r}}_{\mathrm{BL}}} \log_2\left(1 + \frac{\bar{\mathcal{A}}K\mathfrak{p}}{\mathbb{N}_o \mathcal{W}_m}\right) \quad \text{b/s} \tag{6}$$

where $\boldsymbol{\mathcal{r}}_{\mathrm{BL}}$ is defined as the overhead factor, both in time and in frequency, which is required for the BL system to comply with Constraint 2. When $\frac{\bar{\mathcal{A}}K\mathfrak{p}}{N_o \mathcal{W}_m} > 1$, (6) implies that doubling

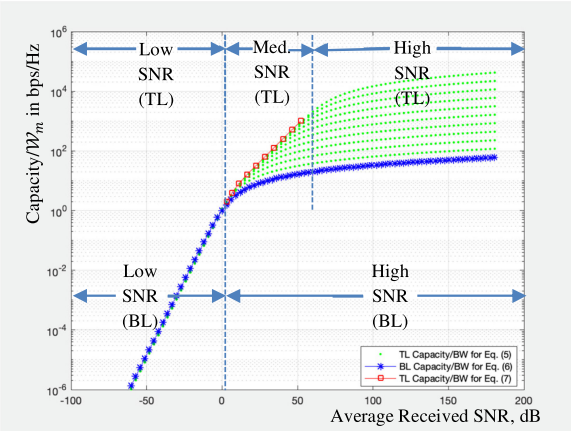

Fig. 1. Comparison of capacity/$\mathcal{W}_m$ between TL and BL systems.

$\mathcal{C}_{\rm BL}$, with a fixed BW, requires a geometric multiple increase in $\frac{\bar{\mathcal{A}}K\mathfrak{p}}{\mathbb{N}_o\mathcal{W}_m}$ since its contribution toward $\mathcal{C}_{\rm BL}$ is logarithmic.

Fig. 1 compares $\mathcal{C}_{\rm TL}/\mathcal{W}_m$ in (5) (shown with green "." markers) with $\mathcal{C}_{\rm BL}/\mathcal{W}_m$ in (6) (shown with blue "$*$" markers) when $\boldsymbol{\mathcal{r}} = \boldsymbol{\mathcal{r}}_{\rm BL} = 1$, $\boldsymbol{\mathcal{d}} = K = 1$ and the kth column, $\{\boldsymbol{h}_{\rm Ch}\}_k$ of $h_{\rm Ch}$ corresponds to a rectangular pulse $\forall k$. In Fig. 1, $\mathcal{C}_{\rm TL}/\mathcal{W}_m$ in (5) is illustrated as a number of curves, each curve corresponding to a value of $N_{\min}$. The selected values are $N_{\min} = 1, 2, 4, \ldots, 1024$, with $N_{\min} = 1$ coinciding with $\mathcal{C}_{\rm BL}/\mathcal{W}_m$ in (6). Similar to $\mathcal{C}_{\rm BL}/\mathcal{W}_m$ in (6) , $\mathcal{C}_{\rm TL}/\mathcal{W}_m$ in (5) contains a "Low" SNR region and a "High" SNR region. Unlike $\mathcal{C}_{\rm BL}/\mathcal{W}_m$ in (6), $\mathcal{C}_{\rm TL}/\mathcal{W}_m$ in (5) also contains a medium-SNR region, denoted as "Med." in Fig. 1 where doubling $\mathcal{C}_{\rm TL}/\mathcal{W}_m$ in (5) requires a fixed multiple increase in $\frac{\Lambda_k\boldsymbol{\mathcal{r}}}{N_{\min}}\frac{\bar{\mathcal{A}}K\mathfrak{p}}{\mathbb{N}_o\mathcal{W}_m}$ since its contribution toward $\mathcal{C}_{\rm TL}$ is mostly linear.

Interpretation of Fig. 1: The medium-SNR region is created in $\mathcal{C}_{\rm TL}$ in (5) when the average received BL SNR, $\frac{\bar{\mathcal{A}}K\mathfrak{p}}{\mathbb{N}_o\mathcal{W}_m}$, is >1 while $\frac{\bar{\mathcal{A}}K\mathfrak{p}}{\mathbb{N}_o\mathcal{W}_m}\frac{\Lambda_k\boldsymbol{\mathcal{r}}}{N_{\min}}$ is $\ll 1$. In other words, $\frac{\Lambda_k\boldsymbol{\mathcal{r}}}{N_{\min}}$ must be much smaller than $\frac{\bar{\mathcal{A}}K\mathfrak{p}}{\mathbb{N}_o\mathcal{W}_m}$ in order to create the medium-SNR region. The source for having Λ_k small and $N_{\min}$ large while keeping $\boldsymbol{\mathcal{r}} < \infty$ is having an arbitrarily large number [9] of complex DOF, while complying with Constraint 2. In a practical design requiring finite latency, all DOF must have a *finite access time* (FAT). We refer to such a set of DOF as FAT, and observe that only TL systems have an arbitrarily large number of FAT DOF in its high-frequency components, whereas BL systems have only a finite number of FAT DOF since it does not contain high-frequency components.

Attribute of $\boldsymbol{h}$ for $\boldsymbol{\mathcal{r}}$ to be $< \infty$: Given that the communication channel in this article is to be constrained by a spectral mask with $\boldsymbol{\mathcal{r}} < \infty$, it is imperative to analyze the PSD, $\mathcal{S}_{x_k(t)}(f)$ of $x_k(t)$. An important attribute of $\boldsymbol{h}$, which affects the spectral decay [17] of $\mathcal{S}_{x_k(t)}(f)$, is the *degree of differenciability* (DOD), $\aleph$, of the kth column, $\{\boldsymbol{h}\}_k$ of $\boldsymbol{h}$, defined as the number of times $\{\boldsymbol{h}\}_k$ can be differenced in time until a Dirac delta impulse δ appears. Mathematically, this implies that $\aleph \triangleq \min_{\{\vec{\Delta}_k^n\}_l=\delta}\{n\}$ where $\{\vec{\Delta}_k^n\}_l$ is the lth element in the differencing vector $\vec{\Delta}_k^n$ of order n, corresponding to $\{\boldsymbol{h}\}_k$, and defined as

$$\left\{\vec{\Delta}_k^n\right\}_l \triangleq \left\{\vec{\Delta}_k^{n-1}\right\}_{l+1} - \left\{\vec{\Delta}_k^{n-1}\right\}_l \text{ for } l \in \{1, \ldots, L-n\}, n \in \mathbb{I}$$

with initial condition: $\{\vec{\Delta}_k^0\}_l \triangleq \{\boldsymbol{h}\}_{k,l}$, $l \in \{1, \ldots, L-1\}$.

Examples of $\aleph$ are as follows:

1) when $\{\boldsymbol{h}\}_k$ is a TL rectangular pulse, $\aleph = 1$;
2) when $\{\boldsymbol{h}\}_k$ is one lobe of a sine wave [2], $\aleph = 2$;
3) when $\{\boldsymbol{h}\}_k$ is a pseudonoise (PN) sequence, $\aleph = 0$.

The following two DOD properties are used below.

1) *DOD Property I:* When $\{\boldsymbol{h}\}_k$ is the sum of two TL vectors, $\{\boldsymbol{h}_1\}_k$ and $\{\boldsymbol{h}_2\}_k$, i.e., $\{\boldsymbol{h}\}_k = \{\boldsymbol{h}_1\}_k + \{\boldsymbol{h}_2\}_k$, with respective DOD, $\aleph_1$ and $\aleph_2$, its resulting DOD $\aleph$ is asymptotically equal to $\lim_{N\to\infty}\aleph = \min(\aleph_1, \aleph_2)$.
2) *DOD Property II:* When $\{\boldsymbol{h}\}_k$ is the linear or circular convolution between two TL vectors, $\{\boldsymbol{h}_1\}_k$ and $\{\boldsymbol{h}_2\}_k$ with respective DOD, $\aleph_1$ and $\aleph_2$, its resulting DOD, $\aleph$, is

$$\aleph = \aleph_1 + \aleph_2.$$

Theorem II derives the slope of the medium-SNR region as a function of the DOD, $\aleph > 0$, of $\boldsymbol{h}_{\rm Ch}$.

Theorem II: Doubling $\mathcal{C}_{\rm TL}$ in (4) across its medium-SNR region requires increasing $\frac{\bar{\mathcal{A}}K\mathfrak{p}}{\mathbb{N}_o f_s}$ by a fixed multiple of $2^{2\aleph}$.

Proof of Theorem II: See Appendix B.

The following constraint derives the modulation, which maximizes $\mathfrak{n}$, when using a minimum mean square error with successive interference cancellation (MMSE-SIC) detector [6, Ch. 8] at Rx, selected for its low complexity and its asymptotic optimality under certain conditions [23]. This constraint maximizes $\mathcal{C}_{\rm TL}$ in the medium-SNR region.

Modulation Constraint: According to [7, p. 6], minimizing the arithmetic mean of the MMSE at Rx is equivalent to maximizing $\frac{d}{d\,\mathrm{SNR}_k}\log_2(1+\frac{\mathrm{SNR}_k}{\boldsymbol{\mathcal{p}}_k})\ \ \forall k$ where SNR_k is the received SNR corresponding to $\{\boldsymbol{h}_{\rm Ch}\}_k$ while $\frac{1}{\boldsymbol{\mathcal{p}}_k}$ is its *multiuser efficiency* [7]. Unlike water-filling [6], which deals with parallel channels, the solution for such optimization is $\frac{\mathrm{SNR}_k}{\boldsymbol{\mathcal{p}}_k} = 1\ \ \forall k$. This implies that the modulation of choice for the elements of $\vec{\alpha}$ is to load each complex DOF by 1 b of information. According to [7], the low-SNR region corresponds to loading <1 b per complex DOF, whereas the high-SNR region typically corresponds to loading >1 b per complex DOF. When $\mathcal{A}_k \neq \bar{\mathcal{A}}$ for some k, we use instead

$$\text{Constraint 3: } \min_k\{\mathrm{SNR}_k\} \geq \max_k\{\boldsymbol{\mathcal{p}}_k\}.$$

Theorem III modifies Theorem I to include a mask constraint and a modulation constraint.

Theorem III: The capacity $\mathcal{C}_{\rm TL}$ of the TL channel corresponding to $\boldsymbol{h}_{\rm Ch}$ in (3), subject to Constraints 1–3, with $K \leq \boldsymbol{\mathcal{d}}$ and with $\aleph > 0$ is

$$\mathcal{C}_{\rm TL} = \frac{\mathcal{W}_m}{\boldsymbol{\mathcal{r}}}\frac{N}{M}\sum_{k=1}^{Q}\log_2\left(1+\frac{\mathrm{SNR}_k}{\boldsymbol{\mathcal{p}}_k}\right)\ \text{bps} \qquad (7)$$

where $\boldsymbol{\mathcal{p}}_k$ is asymptotically $\propto \frac{1}{\boldsymbol{\mathcal{r}}}K^{2\aleph-1}N_{\boldsymbol{\mathcal{d}}}^{2\aleph}$ as $N \gg 1$ with $N_{\boldsymbol{\mathcal{d}}} \triangleq \lceil N/\boldsymbol{\mathcal{d}}\rceil$, the ceiling of $N/\boldsymbol{\mathcal{d}}$, and $N \geq N_{\min}$, using an MMSE-SIC detector at Rx.

Proof of Theorem III: See Appendix C.

Importance of Theorem III is as follows.

In Fig. 1 $\mathcal{C}_{\rm TL}/\mathcal{W}_m$ in (7) is illustrated as a number of points (shown with red "square" markers), each corresponding to a value of $N_{\min}$. Fig. 1 shows that Constraint 3 maximizes $\mathcal{C}_{\rm TL}$ in the medium-SNR region. Based on (7) and Constraint 3, $\lim_{L\to\infty}\mathcal{C}_{\rm TL} \geq \frac{\mathcal{W}_m}{\boldsymbol{\mathcal{r}}}\frac{NK}{\boldsymbol{\mathcal{d}}}$. Therefore, doubling $\lim_{L\to\infty}\mathcal{C}_{\rm TL}$ by doubling $\frac{N}{\boldsymbol{\mathcal{d}}}$, for a fixed $\frac{\mathcal{W}_m}{\boldsymbol{\mathcal{r}}}$ and K, requires increasing SNR_k by a fixed multiple of $2^{2\aleph}$. Similarly, doubling $\lim_{L\to\infty}\mathcal{C}_{\rm TL}$ by

doubling K, for a fixed $\frac{\mathcal{W}_m}{r}$ and $\frac{N}{d}$, requires increasing SNR_k by a fixed multiple of $2^{2\aleph-1}$ as long as $K \leq d$. The next section introduces a novel mask-matched TL system with FAT DOF, referred to as an MTF system.

III. MTF Design

Design Problem: $\boldsymbol{h}$ in (1) is to be designed based on Theorems I and III with the goal of achieving a desired channel capacity $\mathcal{C}_\mathfrak{d}$ for a given channel constrained by a mask $\mathbb{P}_{\mathrm{Mask}}(f)$ of BW $\mathcal{W}_m$. Three design steps, MTF Design Steps I–III, are shown ahead, followed by a proposed MTF design implementation. All three steps attempt to design $\boldsymbol{h}$ such that the minimum required average received SNR is minimized for a given desired capacity $\mathcal{C}_\mathfrak{d}$ and for a given mask $\mathbb{P}_{\mathrm{Mask}}(f)$. This requires designing $\boldsymbol{h}$ s.t. the set $\{\Lambda_k\}_{k=1}^{\mathrm{rank}(\boldsymbol{h}_{\mathrm{Ch}})}$ of squared singular values of $\boldsymbol{h}_{\mathrm{Ch}}$ in (3) has a variance that is minimized while complying with Constraint 2.

MTF Design Solution: First, we define $T_{s,\max} \triangleq \frac{K}{\Delta \mathcal{C}_\mathfrak{d}} \geq 1/f_s$ as a function of K and d, which depends on the selected TL channel. For example, when the TL channel has relatively low interference, such as with $K = 1$, one can select the TL system to be with *memory* [7], i.e., with $d = 1 < N$, implying that $T_{s,\max} = \frac{1}{\mathcal{C}_\mathfrak{d}} \geq 1/f_s$ or $f_s \geq \mathcal{C}_\mathfrak{d}$. On the other hand, when the TL channel has relatively high interference, i.e., with $K \gg 1$, one can select the TL system to be *memoryless* [7], i.e., with $d = N$, implying that $T_{s,\max} = \frac{K}{N\mathcal{C}_\mathfrak{d}} \geq 1/f_s$ or $f_s \geq \frac{N}{K}\mathcal{C}_\mathfrak{d}$.

MTF Design Step I: For a fixed $T_s \leq T_{s,\max}$, select the number N of FAT DOF as $N \triangleq N_\mathcal{S} + N_\mathcal{I}$, where the following statements hold:

1) $N_\mathcal{S}$ is defined as the number of shaping FAT (S-FAT) DOF selected such that $N_\mathcal{S} \geq N_{\min}$ in order to comply with the BW constraint, $\mathcal{W}_{\mathrm{TL}} \leq \mathcal{W}_m$, of $\mathbb{P}_{\mathrm{Mask}}(f)$, whereas
2) $N_\mathcal{I}$ is defined as the number of interpolating FAT (I-FAT) DOF obtained through the creation of interpolated sampled frequencies inside the existing band.

Power is taken from existing frequencies and allocated to the newly formed frequencies s.t. Constraint 1 is preserved.

MTF Design Step II: Once N is selected and the newly sampled frequencies are created, $\boldsymbol{\mathcal{p}}_k$ can be reduced by *equalizing* the power, $E\{|H_k(\Omega)|^2\}$, across $\Omega \in [-\pi, \pi]$ as much as possible, while preserving Constraint 2, where $H_k(\Omega)$ is the discrete-time Fourier transform (DTFT) of the kth column, $\{\boldsymbol{h}\}_k$ of $\boldsymbol{h}$ and Ω is the normalized frequency. This equalization is defined as taking power from frequency samples with *above average* power and allocating it to frequencies with *below average* power, thereby preserving Constraint 1. It can be shown using Karamata's inequality [18] that such power allocation reduces the variance of $\{\Lambda_k\}_{k=1}^{\mathrm{rank}(\boldsymbol{h}_{\mathrm{Ch}})}$ hence increasing $\mathcal{C}_{\mathrm{TL}}$.

MTF Design Step III: Once N is selected, the newly sampled frequencies are created, and the power, $E\{|H_k(\Omega)|^2\}$, across $\Omega \in [-\pi, \pi]$ is equalized as much as possible, $\boldsymbol{\mathcal{p}}_k$ can be reduced by selecting the phase in $H_k(\Omega)$, s.t. the entries of $\boldsymbol{h}$ are zero mean RVs, ideally Gaussian. This assignment of the phase in $H_k(\Omega)$ does not affect the power, $E\{|H_k(\Omega)|^2\}$, across $\Omega \in [-\pi, \pi]$, and thus, preserves Constraints 1 and 2.

Nomenclature: We refer to $\boldsymbol{h}$ designed based on MTF Design Steps I–III, and subject to Constraints 1–3, as an MTF matrix. In this case, we denote $\boldsymbol{h}$ as $\boldsymbol{h}_{\mathrm{MTF}}$, $\boldsymbol{h}_{\mathrm{Ch}}$ as $\boldsymbol{h}_{\mathrm{MTF,Ch}}$, $\boldsymbol{h}_{\mathrm{Basic}}$ as $\boldsymbol{h}_{B\_\mathrm{MTF}}$, and $\mathcal{C}_{\mathrm{TL}}$ in (7) as $\mathcal{C}_{\mathrm{MTF}}$, and refer to the combination of the MTF system and of the channel as the MTF *channel*.

MTF Design Implementation: An implementation of MTF Design Steps I–III is proposed here where the kth column, $\{\boldsymbol{h}_{\mathrm{MTF}}\}_k$, of $\boldsymbol{h}_{\mathrm{MTF}}$, is expressed as a sum

$$\{\boldsymbol{h}_{\mathrm{MTF}}\}_k \triangleq \vec{\wp}_{k,\aleph} + \vec{\wp}_{k,0} \tag{8}$$

of two vectors, $\vec{\wp}_{k,\aleph}$ and $\vec{\wp}_{k,0}$, defined as follows.

Vector I: $\vec{\wp}_{k,\aleph} \in \mathbb{C}^{N\times 1}$ is a pulse vector with a DOD, $\aleph > 0$, selected in order for $\{\boldsymbol{h}_{\mathrm{MTF}}\}_k$ to comply with the BW constraint, i.e., $\mathcal{W}_{\mathrm{TL}} \leq \mathcal{W}_m$, of $\mathbb{P}_{\mathrm{Mask}}(f)$. It is formed using $\aleph$ linear convolutions (each denoted by $*$)

$$\vec{\wp}_{k,\aleph} \triangleq \left(\vec{h}_{1,k} \circledast \vec{g}_{1,k}\right) *, \ldots, * \left(\vec{h}_{\aleph,k} \circledast \vec{g}_{\aleph,k}\right) * \vec{b}_k \tag{9}$$

between $\aleph + 1 > 0$ vectors, with the lth vector, $(\vec{h}_{l,k} \circledast \vec{g}_{l,k})$ for $l \leq \aleph$, formed as a circular convolution (denoted by $\circledast$) between a zero mean PR vector, $\vec{g}_{l,k} \in \mathbb{C}^{N_l \times 1}$ with a $\mathrm{DOD} = 0$, and a vector pulse, $\vec{h}_{l,k} \in \mathbb{C}^{N_l \times 1}$ with a $\mathrm{DOD} = 1$, whereas $\vec{b}_k \in \mathbb{C}^{N_{\aleph+1}\times 1}$ is a zero mean PR vector with a $\mathrm{DOD} = 0$. The first $\aleph - 1$ linear convolutions produce $N_\mathcal{S} \triangleq \sum_{l=1}^{\aleph} N_l - \aleph + 1$ S-FAT DOF, whereas the last produces $N_\mathcal{I} \triangleq N_{\aleph+1} - 1$ I-FAT DOF.

Vector II: $\vec{\wp}_{k,0} \in \mathbb{C}^{N_0 \times 1}$ is a PR vector with a $\mathrm{DOD} = 0$ selected s.t. $\{\boldsymbol{h}_{\mathrm{MTF}}\}_k$ complies with the FOSE constraint of $\mathbb{P}_{\mathrm{Mask}}(f)$, i.e., with a power level $\mathcal{S}_{x_k(t)}(f) \leq \frac{1}{\mathcal{R}}$ in the FOSE band. It is possible to generalize N_0 so that it is not necessarily equal to N. For example, it is possible to select $N_0 = 0$, implying that $\vec{\wp}_{k,0}$ is not included in (8), or equivalently $\{\boldsymbol{h}_{\mathrm{MTF}}\}_k \triangleq \vec{\wp}_{k,\aleph}$. It is also possible to select $N_0 > N$. In this case, $N_0 - N$ zeros must be appended to $\vec{\wp}_{k,\aleph}$ in (9) in order for $\vec{\wp}_{k,\aleph}$ and $\{\boldsymbol{h}_{\mathrm{MTF}}\}_k$ to have a total length of N_0.

The reasoning behind separating $\{\boldsymbol{h}_{\mathrm{MTF}}\}_k$ in (8) into two vectors, $\vec{\wp}_{k,\aleph}$ and $\vec{\wp}_{k,0}$, is that it is difficult to simultaneously comply with the following:

1) the BW constraint, i.e., $\mathcal{W}_{\mathrm{TL}} \leq \mathcal{W}_m$, of the mask; and
2) the FOSE constraint, i.e., $\mathcal{S}_{x_k(t)}(f) \leq \frac{1}{\mathcal{R}}$, of the mask

using a single vector with a single DOD. By taking advantage of DOD Property I, summing $\vec{\wp}_{k,\aleph}$ and $\vec{\wp}_{k,0}$ results in $\{\boldsymbol{h}_{\mathrm{MTF}}\}_k$ having a DOD $\aleph$, since $\vec{\wp}_{k,0}$ has a $\mathrm{DOD} = 0$.

The reasoning behind using circular convolutions in $\vec{\wp}_{k,\aleph}$ in (8) is that it is difficult to use a single vector with a single DOD while achieving the following two requirements:

1) the entries of $\{\boldsymbol{h}_{\mathrm{MTF}}\}_k$ are zero mean RVs, whereas
2) $\{\boldsymbol{h}_{\mathrm{MTF}}\}_k$ complies with the constraint that $\mathcal{W}_{\mathrm{TL}} \leq \mathcal{W}_m$.

By taking advantage of DOD Property II, circularly convolving $\vec{h}_{l,k}$ with $\vec{g}_{l,k}$ produces a vector with a $\mathrm{DOD} = 1$ since the DOD for $\vec{g}_{l,k}$ is 0, implying that $\vec{\wp}_{k,\aleph}$ has a DOD $\aleph$. The pulse $\vec{\wp}_{k,\aleph}$ is made to comply with $\mathcal{W}_{\mathrm{TL}} \leq \mathcal{W}_m$ by properly selecting $\aleph$ and r.

Theorem IV: The MTF channel corresponding to $\{\boldsymbol{h}_{\mathrm{MTF}}\}_k$ in (8) with $N_\mathcal{I} = 0$ under Constraints 1–3, has a capacity $\mathcal{C}_{\mathrm{MTF}}$ identical to $\mathcal{C}_{\mathrm{TL}}$ in (7) except $\boldsymbol{\mathcal{p}}_k$ is proportional to

$$\boldsymbol{\mathcal{p}}_k \propto \left(\frac{1 + \frac{N_0}{\lambda \mathcal{R}}}{\frac{1}{c_{K,N,d,\aleph}\, \frac{1}{r}\, K^{2\aleph-1} N_d^{2\aleph}} + c_{N_0,0}\, \frac{r N_0}{\lambda \mathcal{R} N}}\right) \text{ as } N \gg 1 \tag{10}$$

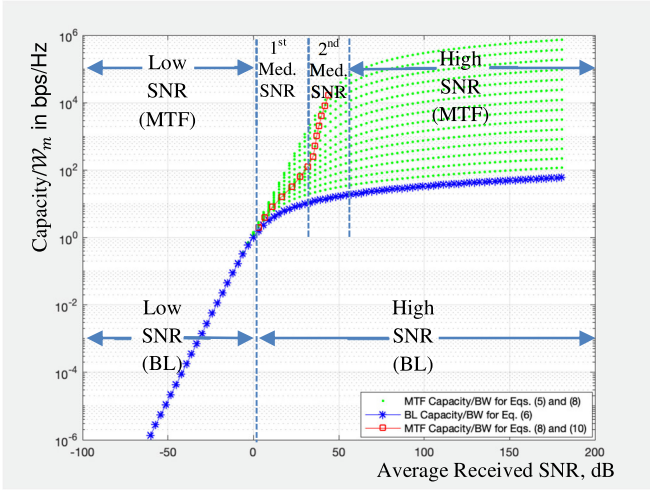

Fig. 2. Comparison of capacity/$\mathcal{W}_m$ between MTF and BL systems.

where $c_{K,N,d,\aleph}$ and $c_{N_0,0}$ are the *coefficients of proportionality* corresponding to $\vec{\varphi}_{k,\aleph}$ and $\vec{\varphi}_{k,0}$ in (8) respectively, with $\lambda \triangleq \mathfrak{p}/\urcorner$, using an MMSE-SIC detector at Rx.

Proof of Theorem IV: See Appendix D.

Importance of Theorem IV. Based on (10), $\mathcal{C}_{\rm MTF}$ consists of two medium-SNR regions, as shown in Fig. 2. As N increases, doubling $\mathcal{C}_{\rm MTF}$ initially requires increasing the SNR by a fixed multiple of $2^{2\aleph}$, which is the first medium-SNR region, referred to as "1st Med." in Fig. 2. Then, later on it requires increasing the SNR by a fixed multiple of 2, which is the second medium-SNR region, referred to as "2nd Med." in Fig. 2. Fig. 2 compares $\mathcal{C}_{\rm MTF}/\mathcal{W}_m$ based on (10) with $\mathcal{C}_{\rm BL}/\mathcal{W}_m$ in (6), where $r = r_{\rm BL} = 1$, $\aleph = 1$, $d = K = 1$, and $\vec{\varphi}_{k,\aleph}$ in (8) is a rectangular pulse with $\vec{\varphi}_{k,0}$ in (8) 30 dBr below $\vec{\varphi}_{k,\aleph}$. In Fig. 2, $\mathcal{C}_{\rm MTF}/\mathcal{W}_m$ without Constraint 3 is illustrated as a number of curves (with green "." markers), each curve corresponding to a value of $N_{\min}$. $\mathcal{C}_{\rm MTF}/\mathcal{W}_m$ with Constraint 3 is illustrated as a number of points (with red "square" markers), each point corresponding to a value of $N_{\min}$. Fig. 2 shows that indeed Constraint 3 maximizes $\mathcal{C}_{\rm MTF}/\mathcal{W}_m$ in both medium-SNR regions.

Under certain conditions, the following asymptotic limits can be reached.

1) When $\frac{N_0}{\lambda\mathcal{R}} \ll 1$, Theorem IV reduces to Theorem III.
2) When $\frac{N_0}{\lambda\mathcal{R}} \gg 1$ and $c_{N_0,0}\frac{rN_0}{\lambda\mathcal{R}N} \gg \frac{1}{c_{K,N,d,\aleph}\,\frac{1}{r}\,K^{2\aleph-1}N_d^{2\aleph}}$, we have

$$\lim_{N_0\to\infty} p_k = \frac{N}{r} \tag{11}$$

This limit applies to the case when $\mathbb{P}_{\rm Mask}(f)$ corresponds to the the IEEE 802.11 WLAN mask, denoted as $\mathbb{P}_{\rm WiFi}(f)$.

3) When $\frac{N_0}{\lambda\mathcal{R}} \triangleq q \ll 1$ with q a constant and $c_{N_0,0}\frac{rN_0}{\lambda\mathcal{R}N} \gg \frac{1}{c_{K,N,d,\aleph}\,\frac{1}{r}\,K^{2\aleph-1}N_d^{2\aleph}}$, we have

$$\lim_{N_0\to\infty} p_k = \frac{N}{qr} \tag{12}$$

This limit applies to the case when $\mathbb{P}_{\rm Mask}(f)$ corresponds to the 3GPP LTE (E-UTRA) mask, denoted as $\mathbb{P}_{LTE}(f)$.

This concludes the theoretical component of this article. Based on such a component, the following two sections design practical MTF systems using realistic constraints.

IV. MTF Architecture

Section IV-A introduces the constraints that are generally imposed on wireless communication systems such as standard-imposed spectral masks, as well as the effects of fading and interference across the wireless channel. Section IV-B proposes several MTF designs based on the constraints introduced in Section IV-A, whereas Section IV-C introduces an architecture that is suitable for allowing various MTF systems to communicate with each other when colocated while using the same band.

A. Design Constraints

First, we select two important $\mathbb{P}_{\rm Mask}(f)$, namely $\mathbb{P}_{\rm WiFi}(f)$ and $\mathbb{P}_{LTE}(f)$. Then, we model the wireless channel and examine its effects on the MTF architecture including the types of interference and restricted bands across such a channel.

Selection of $\mathbb{P}_{\rm Mask}(f)$: In order to include Constraint 2 in Design Steps I–III, and in order to derive a fair comparison with existing systems, we define $\mathbb{P}_{\rm WiFi}(f)$ and $\mathbb{P}_{LTE}(f)$:

1) The IEEE 802.11 WLAN mask for a 20-MHz BW is

$$\mathbb{P}_{\rm WiFi}(f) \triangleq \begin{cases} 0\,\text{dBr} & |f| \le 9\ \text{MHz} \\ \text{line from } 0 \text{ to } -20\,\text{dBr} & 9\ \text{MHz} \le |f| \le 11\ \text{MHz} \\ \text{line from } -20 \text{ to } -28\,\text{dBr} & 11\ \text{MHz} \le |f| \le 20\ \text{MHz} \\ \text{line from } -28 \text{ to } -40\,\text{dBr} & 20\ \text{MHz} \le |f| \le 30\ \text{MHz} \\ -40\,\text{dBr} & 30\ \text{MHz} \le |f|. \end{cases}$$

In $\mathbb{P}_{\rm WiFi}(f)$, the first frequency band, $|f| \le 9$ MHz, corresponds to the occupied band with a BW, $\mathcal{W}_m = 18$ MHz. The middle three frequency bands correspond to OOBE with a BW, $\mathcal{W}_{\rm OOBE} = 42$ MHz. The last frequency band, $|f| \ge 30$ MHz, correspond to the FOSE band with an infinite BW and a power level $1/\mathcal{R} = -40$ dBr.

2) The 3GPP LTE (E-UTRA) mask, $\mathbb{P}_{LTE}(f)$, is defined for a 1.4, 3, 5, 10, 15, and 20 MHz BW, as having $\le$1% OOBE BW, or equivalently, $\mathcal{W}_m$ must contain $\ge$99% of the total integrated mean power in $x_k(t)\ \forall k$.

Modeling of the Wireless Channel: When $f_s \triangleq 1/T_s$ is $\ge$ 8 MHz and $NT_s \le 1$ ms, the wireless channel can be modeled as a frequency-selective slowly fading channel affected by a frequency-dependent PL modeled after Friis free-space PL (FSPL) model [6]. Mathematically, such a channel can be modeled as a linear time-invariant (LTI) system, and characterized using a discrete-time random impulse response $\vec{h}_{\rm Ch}$ of finite length δN referred to as the discrete delay spread of the channel. Moreover, the fading can be modeled either as Rayleigh for a non-LOS channel or as Rician with a strong LOS component for a LOS channel.

Effects of the selected wireless channel model are as follows.

1) Mathematically, the main effect of the frequency-selective channel is to linearly convolve each column $\{\boldsymbol{h}_{\rm MTF}\}_k$ in $\boldsymbol{h}_{\rm MTF}$ with $\vec{h}_{\rm Ch}$. The outcome of such a convolution is a new MTF matrix, $\boldsymbol{h}_{\rm MTF,Ch} \in \mathbb{C}^{\mathcal{M}\times Q}$, defined as

$$\boldsymbol{h}_{\rm MTF,Ch} \triangleq \text{toep}_d\left\{\vec{\boldsymbol{h}}_{\rm MTF,Ch}\right\} \tag{13}$$

where $\vec{\boldsymbol{h}}_{\mathrm{MTF,Ch}} \in \mathbb{C}^{\mathcal{M}\times K}$ has $\boldsymbol{h}_{B\_\mathrm{MTF}}$ replaced by $\boldsymbol{h}_{B\_\mathrm{MTF,Ch}} \in \mathbb{C}^{\mathcal{N}\times K}$ with M replaced by $\mathcal{M} \triangleq \mathcal{N} + \mathcal{d}(L-1)$, N replaced by $\mathcal{N} \triangleq N + \delta N - 1$ and N_o replaced by $\mathcal{N}_o \triangleq N_o + \delta N - 1$. The increase in N and in N_o by $\delta N - 1$ is equivalent to an increase in the number, $N_\jmath$, of I-FAT DOF in the MTF system by δN. Based on DOD Property II, the linear convolution between $\vec{h}_{\mathrm{Ch}}$ and the kth column, $\{\boldsymbol{h}_{\mathrm{MTF}}\}_k$, in $\boldsymbol{h}_{\mathrm{MTF}}$ implies that the resulting DOD is equal to the sum between the original DOD $\aleph$ and the DOD $\aleph_{\mathrm{Ch}}$ of the wireless channel. Based on the adopted frequency-selective fading model of the wireless channel, $\aleph_{\mathrm{Ch}} = 0$. In other words, the resulting DOD of $\boldsymbol{h}_{\mathrm{MTF,Ch}}$ is equal to the original DOD of $\boldsymbol{h}_{\mathrm{MTF}}$ when the wireless channel is frequency-selective.

2) The wireless channel can be equivalently characterized in the frequency domain by the DTFT of $\vec{h}_{\mathrm{Ch}}$, also referred to as its *transfer function* (TF), $H_{\mathrm{Ch}}(\Omega)$. This implies that the following continuous-frequency product:

$$H_{\mathrm{MTF}_k,\mathrm{Ch}}(\Omega) \triangleq H_{\mathrm{MTF}_k}(\Omega)\, H_{\mathrm{Ch}}(\Omega) \quad \forall \Omega \in [-\pi, \pi] \tag{14}$$

can replace the linear discrete-time convolution between $\{\boldsymbol{h}_{\mathrm{MTF}}\}_k$ and $\vec{h}_{\mathrm{Ch}}$ where $H_{\mathrm{MTF}_k,\mathrm{Ch}}(\Omega)$ is the DTFT of the kth column, $\{\boldsymbol{h}_{\mathrm{MTF,Ch}}\}_k$, of $\boldsymbol{h}_{\mathrm{MTF,Ch}}$.

3) Friis FSPL model [6] is based on $E\{|H_{\mathrm{Ch}}(\Omega)|^2\}$ being inversely proportional to $|\Omega|^2$, i.e.,

$$E\left\{|H_{\mathrm{Ch}}(\Omega)|^2\right\} \propto \frac{1}{|\Omega|^2} \quad \forall \Omega \in [-\pi, 0) \cup (0, \pi] \tag{15}$$

where $E\{.\}$ denotes expectation w.r.t. $H_{\mathrm{Ch}}(\Omega)$ at Ω, assuming it is ergodic. Based on (15), it is possible to see that the FSPL has a DOD equal to 1. In other words, the effect of the FSPL is to increase the original DOD $\aleph$ of $\{\boldsymbol{h}_{\mathrm{MTF}}\}_k$ by 1 if the carrier frequency, $f_c = 0$, otherwise, the effect of the FSPL on $\aleph$ depends on f_c.

Based on all effects of the wireless channel, Theorem IV is still valid after replacing $H_{\mathrm{MTF}_k}(\Omega)$ by $H_{\mathrm{MTF}_k,\mathrm{Ch}}(\Omega)$, M by $\mathcal{M}$, and after re-evaluating $\aleph$ based on f_c. In order to preserve the original DOD, $\aleph$, of $\boldsymbol{h}_{\mathrm{MTF}}$ a prechannel filter is required at Tx, which is discussed in Section IV-B.

Modeling of Interference: Two types of interference exist across a wireless network, which are as follows:

1) narrow-band interference (NBI), defined as having a width $\leq$125 MHz;
2) wideband interference (WBI), defined as having a width $>$125 MHz.

NBI encompasses transmissions from existing systems such as LTE and Wi-Fi systems, whereas WBI encompasses transmissions from ultrawideband (UWB) systems and from other MTF systems. Several studies have indicated low utilization of the frequency bands at frequencies >2 GHz, as shown in Table I, which displays the average duty cycle versus frequency range $\leq$7075 MHz based on results in [19] in an urban environment. Table I is consistent with several other studies [20], [21] of urban centers across North America and Europe. All studies indicate an exponential decline in utilization directly proportional to frequency f. We refer to frequency ranges with known *heavy utilization* as $\mathcal{B}_{\mathrm{HU}}$.

TABLE I
AVERAGE UTILIZATION DUTY CYCLE

Frequency range (MHz)	Average duty cycle
75 – 1000	42.00 %
1000 – 2000	13.30 %
2000 – 3000	3.73 %
3000 – 4000	4.01 %
4000 – 5000	1.63 %
5000 – 6000	1.98 %
6000 – 7075	1.78 %

Restricted bands $\mathcal{B}_{\mathrm{RB}}$*:* Further to having to contend with both NBI and WBI, some bands, referred to as $\mathcal{B}_{\mathrm{RB}}$, have been deemed restricted by the regulatory bodies (47 CFR 15.205).

B. Pulse and Filter Design

Based on the knowledge of the statistics of the wireless channel including its model, the types of interference across it and the existence of $\mathcal{B}_{\mathrm{RB}}$, this article designs pulses such as $\vec{h}_{l,k}$, $\vec{\wp}_{k,0}$, $\vec{g}_{l,k}$ as well as filters such as a prechannel filter at Tx, and a postchannel filter at Rx with the goal of optimizing $\mathcal{C}_{\mathrm{MTF}}$ subject to Constraints 1–3.

Design of $\vec{h}_{l,k} \in \mathbb{C}^{N_l\times 1}$*:* A fundamental design for $\vec{h}_{l,k}$ in (9) is a rectangular pulse. Even though it has all its zeros on the unit circle, it is possible to move its zeros away from the unit circle by shifting it in frequency by $1/2N_lT_s$. This shift forms a complex pulse $\vec{h}_{\mathrm{REC},l,k}$ with a real part in the shape of one lobe of a cosine wave and an imaginary part in the shape of a negative lobe of a sine wave. When all $\vec{h}_{l,k}$ $\forall l$ are selected as $\vec{h}_{\mathrm{REC},l,k}$, $\vec{\wp}_{k,\aleph}$ in (9) is denoted as $\vec{\wp}_{\mathrm{REC},\aleph}$. When $\vec{\wp}_{k,\aleph}$ in (9) is selected as $\vec{\wp}_{\mathrm{REC},1}$, $\lambda \triangleq \mathfrak{p}/\urcorner$ in Theorem IV is asymptotically equal to π. In this case, the amplitude of $\vec{\wp}_{\mathrm{REC},1}$ is selected to comply with Constraint 1.

Design of $\vec{\wp}_{k,0} \in \mathbb{C}^{N_0\times 1}$*:* A possible design of $\vec{\wp}_{k,0}$ in (8) is

$$\vec{\wp}_{k,0} = \sqrt{\urcorner/\mathcal{R}}\,\mathcal{DFT}^{-1}\left\{\left[\, e^{j\vartheta_{k,1}} \;\cdots\; e^{j\vartheta_{k,N_0}} \,\right]^T\right\} \tag{16}$$

where $\mathcal{DFT}^{-1}$ denotes an inverse discrete Fourier transform (DFT) operation; and the phase, $\vartheta_{k,i} \in \{0, 2\pi\}$, is chosen as PR with a uniform distribution across $\{0, 2\pi\}$ for $1 \leq i \leq N_0$. $\vec{\wp}_{k,0}$ is also known as a frequency-based PR *polyphase* signature.

Design of $\overrightarrow{g}_{l,k} \in \mathbb{C}^{N_l\times 1}$*:* A possible design of $\overrightarrow{g}_{l,k}$ in (9) is

$$\overrightarrow{g}_{l,k} = \mathcal{DFT}^{-1}\left\{\left[\, e^{j\vartheta_{l,k,1}} \;\cdots\; e^{j\vartheta_{l,k,N_l}} \,\right]^T\right\} \tag{17}$$

with the phase, $\vartheta_{l,k,i} \in \{0, 2\pi\}$, chosen as PR with a uniform distribution across $\{0, 2\pi\}$ for $1 \leq i \leq N_l$, similar to $\vec{\wp}_{k,0}$ in (16), except that $\vartheta_{l,k,1}$ must equal ϑ_{l,k,N_l} in order to minimize the overhead factor $\mathrel{r}$. Since the wireless channel forces $H_{\mathrm{MTF}_k}(\Omega)$ in (14) to be multipled by $H_{\mathrm{Ch}}(\Omega)$, the resulting product $H_{\mathrm{MTF}_k,\mathrm{Ch}}(\Omega)$ forces $\overrightarrow{g}_{l,k}$ in (17) to be replaced by

$$\overrightarrow{g}_{l,k,\mathrm{Ch}} = \mathcal{DFT}^{-1}\left\{\left[\, |a_{l,k,1}|\, e^{j\vartheta_{l,k,1}} \;\cdots\; |a_{l,k,\mathcal{N}_l}|\, e^{j\vartheta_{l,k,N_l}} \,\right]^T\right\} \tag{18}$$

when $N_i = 1$ and $\aleph = 1$ where $|a_{l,k,1}|, \ldots, |a_{l,k,\mathcal{N}_l}|$ are random amplitudes, which have either a Rician distribution with

a strong LOS component across a LOS channel, or a Rayleigh distribution across a NLOS channel, and $\mathcal{N}_l \triangleq N_l + \delta N - 1$.

Selection of q when $\mathbb{P}_{\text{Mask}}(f) \equiv \mathbb{P}_{LTE}(f)$: This article selects q in (12) as 0.5% and allocates the remaining 0.5% to the OOBE BW in $\vec{\wp}_{k,\aleph}$. Under Constraint 2, (12) can be rewritten as $\lim_{N_0\to\infty} \boldsymbol{\wp}_k = (N/\boldsymbol{\mathcal{r}})_{\text{dB}} + 23$ dB.

Design of prechannel filtering at Tx: In order to comply with $\mathcal{B}_{\text{RB}}$ (47 CFR 15.205), and to prevent transmitting across $\mathcal{B}_{\text{HU}}$, a prechannel filter is recommended at Tx. Furthermore, according to (15), the effect of the FSPL is to increase the DOD $\aleph$ of $\boldsymbol{h}_{\text{MTF}}$ by 1 despite the fact that $\vec{\wp}_{k,0}$ has been added in (8) to force the resulting DOD to asymptotically take the value 0. In order to address all 3 concerns, $\boldsymbol{h}_{\text{MTF}}$ is replaced by a prechannel MTF matrix $\boldsymbol{h}^{\mathcal{P}}_{\text{MTF}}$ based on replacing in (8) $\vec{\wp}_{k,\aleph}$ by $\vec{\wp}^{\mathcal{P}}_{k,\aleph}$, $\vec{\wp}_{k,0}$ by $\vec{\wp}^{\mathcal{P}}_{k,0}$, and $\{\boldsymbol{h}_{\text{MTF}}\}_k$ by $\{\boldsymbol{h}^{\mathcal{P}}_{\text{MTF}}\}_k \triangleq \vec{\wp}^{\mathcal{P}}_{k,\aleph} + \vec{\wp}^{\mathcal{P}}_{k,0}$ with a DTFT $H^{\mathcal{P}}_{\text{MTF}_k}(\Omega)$ preprocessed by the following two actions:

1) Predistort $H^{\mathcal{P}}_{\text{MTF}_k}(\Omega)$ by $|\Omega|$ $\forall \Omega \in [-\pi, 0) \cup (0, \pi]$ as

$$H^{\mathcal{P}}_{\text{MTF}_k}(\Omega) = \frac{|\Omega|}{\sqrt{\nu}} H_{\text{MTF}_k}(\Omega) \;\; \forall \Omega \in [-\pi, 0) \cup (0, \pi] \tag{19}$$

where ν is selected to keep $E\{|H^{\mathcal{P}}_{\text{MTF}_k}(\Omega)|^2\} \leq \frac{1}{\mathcal{R}}$ $\forall \Omega \in [-\pi, 0) \cup (0, \pi]$.

2) Force $H^{\mathcal{P}}_{\text{MTF}_k}(\Omega)$ to contain a null at the excluded band: $\mathcal{B}_{\text{ex}} \triangleq \{\{\mathcal{B}_{\text{RB}} \cup \mathcal{B}_{\text{HU}}\} \cap \mathcal{B}_{\text{TL}}\} \cup \bar{\mathcal{B}}_{\text{TL}}$ with $\mathcal{B}_{\text{HU}} \triangleq [0, 2\text{ GHz}]$ and $\bar{\mathcal{B}}_{\text{TL}}$ the complement of $\mathcal{B}_{\text{TL}} \triangleq [f_c - f_s/4, f_c + f_s/4]$ and $f_c \geq f_s/4$.

As a result of both actions, $\boldsymbol{\wp}_k$ in (10) is replaced by

$$\boldsymbol{\wp}_k \propto \left(\frac{1 + \frac{N_0}{\lambda \nu \mathcal{R}}}{\frac{1}{c_{K,N,d,\aleph}} \frac{1}{\boldsymbol{\mathcal{r}}} K^{2\aleph-1} N_d^{2\aleph}} + c_{N_0,0} \frac{\boldsymbol{\mathcal{r}} N_0}{\lambda \nu \mathcal{R} N} \right) \text{ as } N \gg 1 \tag{20}$$

and (11) is replaced by $\lim_{N_0\to\infty} \boldsymbol{\wp}_k \to (\frac{N}{\boldsymbol{\mathcal{r}}})_{\text{dB}} - 5.16$ dB since $\nu = 2(\pi^2/6)$ according to Basel problem [22] where $2(\lim_{N_0\to\infty} \sum_{n=1}^{N_0} \frac{1}{n^2}) = 2(\pi^2/6) = 5.16$ dB when the samples are real. On the other hand, (12) is replaced by $\lim_{N_0\to\infty} \boldsymbol{\wp}_k = (\frac{N}{\boldsymbol{\mathcal{r}}})_{\text{dB}} - (q)_{\text{dB}} - 5.16$ dB. For example, when $q = 0.5\%$, $\lim_{N_0\to\infty} \boldsymbol{\wp}_k = (\frac{N}{\boldsymbol{\mathcal{r}}})_{\text{dB}} + 17.9$ dB.

Design of Postchannel filtering at Rx: Postchannel filtering can be used at Rx to reduce the effects of NBI across the wireless channel. In this case, it must include an excision filter, which consists of the following two steps.

1) Estimate the frequency range $\mathcal{B}_{\text{NBI}}$ corresponding to NBI.A frequency f belongs to $\mathcal{B}_{\text{NBI}}$ when $\mathcal{S}_{y(t)}(f) \geq \mathcal{S}_{x_k(t)}(f) + \mathcal{S}_{\text{th}}$ where $\mathcal{S}_{\text{th}}$ is a threshold selected to meet a certain optimization criterion for reducing NBI.
2) Excise the estimated NBI by forcing a null in the PSD $\mathcal{S}_{y(t)}(f)$ of the continuous-time version $y(t)$ of $\vec{y}$ at $f \in \mathcal{B}_{\text{NBI}}$.

Postchannel filtering should also include a null at $\mathcal{B}_{\text{NBI}} \cup \mathcal{B}_{\text{ex}} \triangleq \{\{\mathcal{B}_{\text{NBI}} \cup \mathcal{B}_{\text{RB}} \cup \mathcal{B}_{\text{HU}}\} \cap \mathcal{B}_{\text{TL}}\} \cup \bar{\mathcal{B}}_{\text{TL}}$ in order to reduce the effect of noise and interference at Rx.

Selection of Sampling Type and frequency f_s: There are three types of sampling available in wireless systems: baseband sampling, IF sampling, and RF sampling. RF sampling is recommended when $f_s \geq 4f_c$, since it does not require any up-conversion/down-conversation stages. On the other hand, IF sampling is recommended when $f_s < 4f_c$ since it requires a smaller number of conversion stages compared to baseband sampling. In this case, the intermediate frequency f_{IF} is selected equal to $f_s/4$.

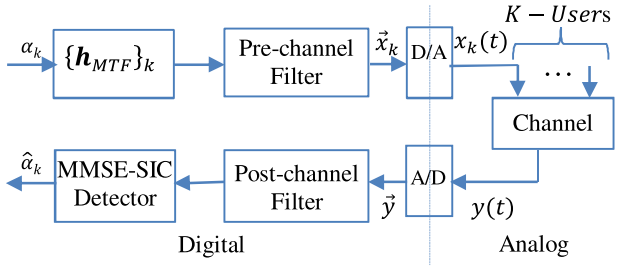

Fig. 3. MTF system architecture.

Selection of Carrier Frequency f_c: In order to select a frequency range s.t. $f_c \leq f_s/4$ with low interference and low PL, while allowing for a multipath-rich environment that is suitable for MIMO communications and while avoiding $\mathcal{B}_{\text{HU}}$, this article proposes to select $f_c \in$ [2 GHz, 6 GHz].

C. MTF System Architecture

The architecture shown in Fig. 3 allows for an MTF system to communicate with other colocated MTF systems, when using the same band, such as cellular-type MTF systems, Wi-Fi-type MTF systems, and wireless sensor/Internet-of-Things-type MTF systems. In Fig. 3, the digital side is software-defined, whereas the analog side is based on a generic hardware, which includes converters [e.g., digital-to-analog (D/A), up/down and analog-to-digital (A/D)], analog filters [e.g., bandpass filter (BPF) and low-pass filter (LPF)] and amplifiers [e.g., power amplifier (PA) and low-noise amplifier (LNA)]. The software-defined side allows any MTF system to change personality according to the MTF system it is communicating with, by adjusting $\{\boldsymbol{h}_{\text{MTF}}\}_k$, pre and postchannel filters as well as the MMSE-SIC detector.

V. MTF MA Networks

This section designs MTF MA networks across a centralized topology similar to existing MA networks, such as LTE and Wi-Fi networks, in order to draw a fair comparison between the two. As typical of any centralized network, the MTF MA network consists of two types of transmissions: 1) downlink (DL) transmissions, from a base station (BS) or access point (AP) to device; and 2) uplink (UL) transmissions, from device to BS/AP. The designs of the MTF MA networks are based on the following assumptions.

A. Assumptions

1) This article assumes that several colocated centralized MTF MA networks use the same band. Based on the system architecture in Section IV, most such networks are able to collaborate in such a way that time division duplex (TDD) can be implemented. TDD is desirable since it forces temporal separation between DL and UL transmissions. On the other hand, this article assumes that it is only possible to realistically maintain limited synchronization and limited power control between each device and the BS/AP it is communicating with. This article assumes that the limited device-level timing synchronization allows

for separation between most DL and UL transmissions, whereas the limited device-level power control assumes most UL transmissions, which are received at their designated BS/AP within ± 6 dB. This assumption justifies qualifying the UL portion of most of the MTF MA networks as of *relatively high interference*.

2) This article assumes that an MTF BS/AP contains an antenna array. However, it is unlikely that an MTF device does. This article also assumes that each MTF BS/AP has knowledge of the angles of arrival of transmissions from its MTF devices. For this reason, this article proposes to use beamforming in the DL portion of most of the MTF MA networks in order to reduce WBI from interfering BSs/APs at the MTF devices. This article assumes that beamforming at Tx of the BS/AP in its DL portion is capable of offering a 16 dBi antenna gain to any device (as allowed under the FCC's Title 47 CFR 15.247 for a point-to-point transmission), hence forcing transmissions from interfering MTF BSs/APs at a device to be reduced by ≥ 10 dB relative to transmissions from the designated BS/AP. This reduction in transmissions from interfering MTF BSs/APs at an MTF device justifies qualifying its DL portion as of *relatively low interference*.
3) This article assumes that the range $\Re_k$ between the kth MTF Tx and an MTF Rx is a function of the link budget $\mathfrak{L}_k$ between them, where

$$\mathfrak{L}_{k,\mathrm{dB}} \triangleq \mathfrak{p}_{\mathrm{dBm}} - NF_{\mathrm{dB}} - (\mathbb{N}_o \mathcal{W}_m)_{\mathrm{dB}} - \max_k \left\{\boldsymbol{\rho}_k^{\mathcal{P}}\right\}_{\mathrm{dB}} + G_{\mathrm{dB}}. \tag{21}$$

$\mathfrak{p}_{\mathrm{dBm}}$ is the average transmitted power constrained to be $30\ \mathrm{dBm}$ for DL (as allowed under the FCC's Title 47 CFR 15.247) and 20 dBm for UL. $\mathrm{NF}_{\mathrm{dB}}$ is the noise figure of Rx assumed to be 5 dB. $\boldsymbol{\rho}_k^{\mathcal{P}}$ corresponds to $f_s^{\mathcal{P}} \triangleq f_s(1-\zeta_{\mathrm{ex}})$, which is the noise-equivalent BW in hertz at the output of the postchannel filter. ζ_{ex} is the *excision factor*, defined as $\zeta_{\mathrm{ex}} \triangleq \frac{1}{f_s}\int_{f\in\mathcal{B}_{\mathrm{ex}}} f df$. G_{dB} is the antenna gain between Tx and Rx, assumed to be $16\,\mathrm{dBi}$ at Tx for DL and 0 dBi for UL.
4) This article assumes that the range $\Re_k$ depends on $\mathfrak{L}_{k,\mathrm{dB}}$ based on Friis formulae [6] as follows:

$$\Re_k = 2^{(\mathfrak{L}_{k,\mathrm{dB}} - \mathfrak{L}_{\mathrm{dB},0})/\gamma_{k,\mathrm{dB}}} \tag{22}$$

where $\mathfrak{L}_{\mathrm{dB},0}$ is the PL in dB for reaching 1 m and γ_k is the PL per octave, which depends on the type of fading across the wireless channel. This article assumes that $\gamma_{k,\mathrm{dB}} = 6$ dB/octave in a LOS channel modeled as Rician with a strong LOS component, whereas $\gamma_{k,\mathrm{dB}} = 8$ dB/octave in a NLOS channel modeled as Rayleigh.
5) This article assumes the following.
   a) In (9), $\vec{h}_{1,k} = \cdots = \vec{h}_{\aleph,k}$ and $\overrightarrow{g}_{1,k} = \cdots = \overrightarrow{g}_{\aleph,k}\ \forall k$.
   b) The same $\vec{h}_{l,k}$ in (9) is selected for all MTF devices.
   c) A unique $\overrightarrow{g}_{l,k}$ as defined in (17) and a unique $\vec{\wp}_{k,0}$ as defined in (16) are selected for the kth MTF device $\forall k$.
   d) $\vec{\wp}_{k,\aleph}^{\mathcal{P}}$ has a PSD, $\mathcal{S}_{\wp_{k,\aleph}^{\mathcal{P}}(t)}(f)$, with nulls at $\mathcal{B}_{\mathrm{NBI}} \cup \mathcal{B}_{\mathrm{ex}}$, $\wp_{k,\aleph}^{\mathcal{P}}(t)$ being the continuous-time version of $\vec{\wp}_{k,\aleph}^{\mathcal{P}}$.
   e) $\vec{\wp}_{k,0}^{\mathcal{P}}$ has a PSD, $\mathcal{S}_{\wp_{k,0}^{\mathcal{P}}(t)}(f)$, predistorted according to (19), $\wp_{k,0}^{\mathcal{P}}(t)$ being the continuous-time version of $\vec{\wp}_{k,0}^{\mathcal{P}}$.
   f) Rx includes an MMSE-SIC detector.
6) This article assumes that $\mathcal{d}|_{\mathrm{UL}} = N$ in the UL portion of an MTF MA network in order to decrease $\max_k\{\boldsymbol{\rho}_k\}$ in (21), whereas it assumes that $\mathcal{d}|_{\mathrm{DL}} = 1$ in the DL portion in order to maintain a high DL capacity, $\mathcal{C}_{\mathrm{MTF}}$, where $\mathcal{d}|_{\mathrm{UL}}$ and $\mathcal{d}|_{\mathrm{DL}}$ are the delays in (2) corresponding to UL and DL, respectively. An additional reason for selecting $\mathcal{d}|_{\mathrm{UL}} = N$ is to reduce the peak-to-average power ratio (PAPR) corresponding to transmissions from an MTF device, which can be reduced even further by selecting $\vec{\wp}_{k,\aleph}$ in (9) as $\vec{\wp}_{\mathrm{REC},1}$. A further reason for selecting $\mathcal{d}|_{\mathrm{UL}} = N$ is to have a memoryless MTF MA network with $\mathcal{C}_{\mathrm{MTF}}|_{L<\infty} = \mathcal{C}_{\mathrm{MTF}}$. On the other hand, selecting $\mathcal{d}|_{\mathrm{DL}} = 1$ in the DL portion implies that the MTF MA network has memory and $\mathcal{C}_{\mathrm{MTF}}|_{L<\infty} = L/(L + \frac{N}{\mathcal{d}} - 1)\mathcal{C}_{\mathrm{MTF}}$. For example, when $10N < L < \infty$, $\mathcal{C}_{\mathrm{MTF}} > 0.9\ \mathcal{C}_{\mathrm{MTF}}$.
7) In the UL portion, all Q symbols in $\vec{\alpha}$, corresponding to all the K active Txs, are required to be detected, whereas in the DL portion, only the desired symbols in $\vec{\alpha}$, corresponding to the desired Tx, are required to be detected, with the remaining symbols, corresponding to the $K_{\mathrm{i}} = K - 1$ interfering columns in $\boldsymbol{h}_{\mathrm{MTF}}$, ignored. For this reason, this article constrains $\max_k\{\boldsymbol{\rho}_k\}$ in (21) to correspond to a full implementation of Constraint 3 $\forall k$ for the UL portion, whereas in the DL portion, this article constrains $\max_k\{\boldsymbol{\rho}_k\}$ in (21) to correspond to a partial implementation of Constraint 3 corresponding only to the desired received symbols in $\vec{\alpha}$.

B. Examples of MTF MA Networks

Based on the earlier assumptions, we design three MTF MA networks, namely MTF_1, MTF_2, and MTF_3, all constrained by a mask with a BW, $\mathcal{W}_m = 20$ MHz. This implies that $(NT_s)_{\min} \triangleq \boldsymbol{\tau}/20\ \mu$s. For example, when $\mathbb{P}_{\mathrm{Mask}}(f)$ is selected as $\mathbb{P}_{\mathrm{WiFi}}(f)$ and $\vec{\wp}_{k,\aleph}^{\mathcal{P}}$ as $\vec{\wp}_{\mathrm{REC},1}^{\mathcal{P}}$, $\boldsymbol{\tau} = 64/3 = 21.3$ and $(NT_s)_{\min} \triangleq \boldsymbol{\tau}/20\ \mu\mathrm{s} = 1.066\ \mu$s. On the other hand, when $\mathbb{P}_{\mathrm{Mask}}(f)$ is selected as $\mathbb{P}_{LTE}(f)$ and $\vec{\wp}_{k,\aleph}^{\mathcal{P}}$ as $\vec{\wp}_{\mathrm{REC},1}^{\mathcal{P}}$, $\boldsymbol{\tau} = 40.8$ and $(NT_s)_{\min} \triangleq \boldsymbol{\tau}/20\ \mu\mathrm{s} = 2.04\ \mu$s.

Moreover, since the DL portion of each network is assumed to have relatively low interference, it is characterized to be with memory, with $\mathcal{d} = K = 1$, and $T_{s,\max}|_{\mathrm{DL}} \triangleq 1/\mathcal{C}_{\mathfrak{d}}|_{\mathrm{DL}} \geq 1/f_s|_{\mathrm{DL}}$. On the other hand, since the UL portion of each network is assumed to have relatively high interference, it is characterized as memoryless, with $\mathcal{d} = N$, $K \gg 1$, and $T_{s,\max}|_{\mathrm{UL}} \triangleq \frac{K}{N\,\mathcal{C}_{\mathfrak{d}}|_{\mathrm{UL}}} \geq 1/f_s|_{\mathrm{UL}}$. Therefore, $N_{\min}|_{\mathrm{DL}} \triangleq \frac{(NT_s)_{\min}}{T_{s,\max}|_{\mathrm{DL}}} = \frac{\boldsymbol{\tau}\,\mathcal{C}_{\mathfrak{d}}|_{\mathrm{DL}}}{20\ \mathrm{MHz}}$ and $N_{\min}|_{\mathrm{UL}} \triangleq \frac{(NT_s)_{\min}}{T_{s,\max}|_{\mathrm{UL}}} = \frac{\boldsymbol{\tau}\,\mathcal{C}_{\mathfrak{d}}|_{\mathrm{UL}} N}{20\ \mathrm{MHz}\ K}$.

Design Parameters for MTF_1, MTF_2, and MTF_3 are as follows.

1) MTF_1 is selected to have a desired DL channel capacity of $\mathcal{C}_{\mathfrak{d}_1}|_{\mathrm{DL}} = 0.2$ Gb/s, and a desired UL channel capacity of $\mathcal{C}_{\mathfrak{d}_1}|_{\mathrm{UL}} = 0.2$ Gb/s, both across the unlicensed (Title 47 CFR 15.247) mid-band frequency of $f_{c_1} = 2.45$ GHz. We also select for both DL and UL, $f_{s_1}|_{\mathrm{DL}} = f_{s_1}|_{\mathrm{UL}} = 0.2$ GHz and IF sampling with $\mathcal{B}_{\mathrm{TL}_1} \triangleq [f_{c_1} - f_{s_1}/4, f_{c_1} + \frac{f_{s_1}}{4}]$ and $\mathcal{B}_{\mathrm{ex}_1} \triangleq \{\{\mathcal{B}_{\mathrm{NBI}_1} \cup \mathcal{B}_{\mathrm{RB}} \cup \mathcal{B}_{\mathrm{HU}}\} \cap \mathcal{B}_{\mathrm{TL}_1}\} \cup \bar{\mathcal{B}}_{\mathrm{TL}_1}$.
2) MTF_2 is selected to have $\mathcal{C}_{\mathfrak{d}_2}|_{\mathrm{DL}} = 2$ Gb/s and $\mathcal{C}_{\mathfrak{d}_2}|_{\mathrm{UL}} = 2$ Gb/s, both across the unlicensed

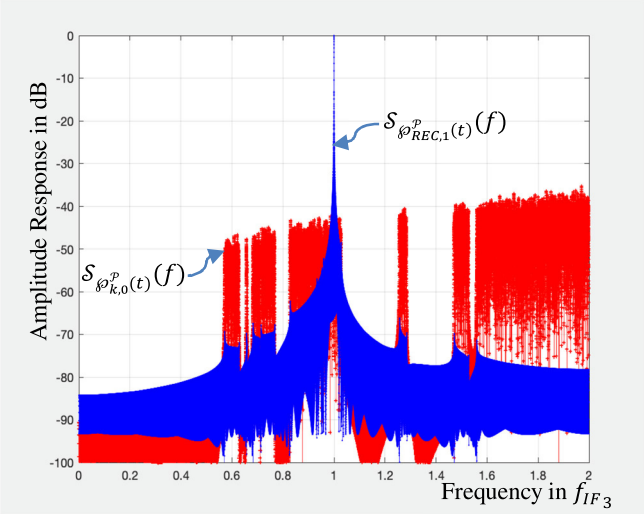

Fig. 4. $\mathcal{S}_{\vec{\wp}^{\mathcal{P}}_{\mathrm{REC},1}(t)}(f)$ and $\mathcal{S}_{\vec{\wp}^{\mathcal{P}}_{k,0}(t)}(f)$ for MTF_3.

mid-band frequency of $f_{c_2} = 5.8$ GHz. We also select $f_{s_2}|_{\mathrm{DL}} = f_{s_2}|_{\mathrm{UL}} = 2$ GHz and IF sampling with $\mathcal{B}_{\mathrm{TL}_2} \triangleq [f_{c_2} - f_{s_2}/4, f_{c_2} + f_{s_2}/4]$ and $\mathcal{B}_{\mathrm{ex}_2} \triangleq \{\{\mathcal{B}_{\mathrm{NBI}_2} \cup \mathcal{B}_{\mathrm{RB}} \cup \mathcal{B}_{\mathrm{HU}}\} \cap \mathcal{B}_{\mathrm{TL}_2}\} \cup \mathcal{B}_{\mathrm{TL}_2}$.

3) MTF_3 uses a licensed band at $f_{c_3} = 3.5$ GHz with $\mathcal{C}_{\mathfrak{d}_3}|_{\mathrm{DL}} = 14$ Gb/s and $\mathcal{C}_{\mathfrak{d}_1}|_{\mathrm{UL}} = 6$ Gb/s. We also select $f_{s_3}|_{\mathrm{DL}} = f_{s_3}|_{\mathrm{UL}} = 14$ GHz and RF sampling with $\mathcal{B}_{\mathrm{TL}_3} \triangleq [f_{c_3} - f_{s_3}/4, f_{c_3} + f_{s_3}/4]$ and $\mathcal{B}_{\mathrm{ex}_3} \triangleq \{\{\mathcal{B}_{\mathrm{NBI}_3} \cup \mathcal{B}_{\mathrm{RB}} \cup \mathcal{B}_{\mathrm{HU}}\} \cap \mathcal{B}_{\mathrm{TL}_3}\} \cup \mathcal{B}_{\mathrm{TL}_3}$.

Fig. 4 displays the PSD, $\mathcal{S}_{\vec{\wp}^{\mathcal{P}}_{\mathrm{REC},1}(t)}(f)$, of $\vec{\wp}^{\mathcal{P}}_{\mathrm{REC},1}$ and the PSD, $\mathcal{S}_{\vec{\wp}^{\mathcal{P}}_{k,0}(t)}(f)$, of $\vec{\wp}^{\mathcal{P}}_{k,0}$ for MTF_3, with nulls at $\mathcal{B}_{\mathrm{ex}_3}$, when $\vec{\wp}^{\mathcal{P}}_{k,\aleph}$ is selected as $\vec{\wp}^{\mathcal{P}}_{\mathrm{REC},1}$ while $\vec{\wp}^{\mathcal{P}}_{k,0}$ is selected as defined in (16) predistorted according to (19). It is possible to increase $\mathcal{C}_{\mathfrak{d}}|_{\mathrm{DL}}$ arbitrarily by decreasing $T_s \triangleq 1/f_{s_3}$ regardless of the value of $\mathcal{W}_m$ at the cost of an increase in $\mathcal{P}_k$.

The Coefficient of Proportionality $c_{K,N,d,\aleph}$ is discussed in the following.

1) Tables II and III summarize the ratio $c_{K,2N,d,\aleph}/c_{K,N,d,\aleph}$ and $\mathcal{r}$ for a number of $\vec{\wp}_{k,\aleph}$, with $K = 1$ and $N_0 = 0$, corresponding to MTF_1 or MTF_2, and MTF_3, respectively. In Tables II and III, $\vec{\wp}^{\mathcal{P},\mathrm{Ric}}_{\mathrm{REC},\aleph}$ denotes a predistorted vector, $\vec{\wp}^{\mathcal{P}}_{\mathrm{REC},\aleph}$, with nulls at $\mathcal{B}_{\mathrm{ex}_1}$ or $\mathcal{B}_{\mathrm{ex}_2}$, and $\mathcal{B}_{\mathrm{ex}_3}$, respectively, transmitted across a frequency-selective Rician fading channel with a strong LOS component, whereas $\vec{\wp}^{\mathcal{P},\mathrm{Ray}}_{\mathrm{REC},\aleph}$ denotes a predistorted vector $\vec{\wp}^{\mathcal{P}}_{\mathrm{REC},\aleph}$ with nulls at $\mathcal{B}_{\mathrm{ex}_1}$ or $\mathcal{B}_{\mathrm{ex}_2}$, and $\mathcal{B}_{\mathrm{ex}_3}$, respectively, transmitted across a frequency-selective Rayleigh fading channel. Both channels are based on the frequency-selective model in (14). According to Tables II and III, when $\aleph = 1, 2$, or 3, SNR_k must be asymptotically increased by 3, 9, or 15 dB, respectively, for every doubling of N_d, with $\vec{\wp}^{\mathcal{P},\mathrm{Ray}}_{\mathrm{REC},\aleph}$ offering a respective saving in SNR_k of up to 6, 18, or 30 dB compared to $\vec{\wp}^{\mathcal{P},\mathrm{Ric}}_{\mathrm{REC},\aleph}$ for $\aleph = 1,\ 2,\ 3$.

2) Table IV shows $c_{K,\mathcal{N},N,1}/c_{1,N,1,1}$ for various values of $\frac{K}{N_{\overline{\mathrm{ex}}}}$ for the UL portion of a centralized MA network where $N_{\overline{\mathrm{ex}}} \triangleq N(1 - \zeta_{\mathrm{ex}})$. In Table IV, $c_{1,N,1,1}$ corresponds to

TABLE II
$\mathcal{r}$ AND $c_{1,N,d,\aleph}$ FOR MTF_1, MTF_2 WITH $K = 1$, $N_0 = 0$

	$\vec{\wp}^{\mathcal{P},Ric}_{REC,1}$	$\vec{\wp}^{\mathcal{P},Ric}_{REC,2}$	$\vec{\wp}^{\mathcal{P},Ric}_{REC,3}$	$\vec{\wp}^{\mathcal{P},Ray}_{REC,1}$	$\vec{\wp}^{\mathcal{P},Ray}_{REC,2}$	$\vec{\wp}^{\mathcal{P},Ray}_{REC,3}$
$\mathcal{r}$ for $\mathbb{P}_{WiFi}(f)$	21.3	3.7	3.1	21.3	3.7	3.1
$\mathcal{r}$ for $\mathbb{P}_{LTE}(f)$	40.8	3.9	3.4	40.8	3.9	3.4
$c_{1,2,d,\aleph}/c_{1,1,d,\aleph}\vert_{dB}$	−2.6	−8.8	−15.2	−3.0	−8.8	−14.8
$c_{1,4,d,\aleph}/c_{1,2,d,\aleph}\vert_{dB}$	−2.6	−8.6	−14.1	−3.0	−9.0	−15.1
$c_{1,8,d,\aleph}/c_{1,4,d,\aleph}\vert_{dB}$	−1.1	−7.3	−14.0	−2.6	−8.8	−14.7
$c_{1,16,d,\aleph}/c_{1,8,d,\aleph}\vert_{dB}$	−0.9	−5.8	−14.1	−2.6	−8.6	−14.2
$c_{1,32,d,\aleph}/c_{1,16,d,\aleph}\vert_{dB}$	−0.8	−5.8	−10.0	−2.6	−7.3	−13.5
$c_{1,64,d,\aleph}/c_{1,32,d,\aleph}\vert_{dB}$	−0.1	−2.8	−7.0	−1.1	−5.8	−12.3
$c_{1,128,d,\aleph}/c_{1,64,d,\aleph}\vert_{dB}$	−0.1	−1.5	−0.7	−0.9	−5.6	−7.3
$c_{1,256,d,\aleph}/c_{1,128,d,\aleph}\vert_{dB}$	−0.	−0.	−0.7	−0.8	−2.8	−5.6
$c_{1,512,d,\aleph}/c_{1,256,d,\aleph}\vert_{dB}$	−0.	−0.	−0.1	−0.1	−1.5	−2.6

TABLE III
$\mathcal{r}$ AND $c_{1,N,d,\aleph}$ FOR MTF_3 WITH $K = 1$ AND $N_0 = 0$

	$\vec{\wp}^{\mathcal{P},Ric}_{REC,1}$	$\vec{\wp}^{\mathcal{P},Ric}_{REC,2}$	$\vec{\wp}^{\mathcal{P},Ric}_{REC,3}$	$\vec{\wp}^{\mathcal{P},Ray}_{REC,1}$	$\vec{\wp}^{\mathcal{P},Ray}_{REC,2}$	$\vec{\wp}^{\mathcal{P},Ray}_{REC,3}$
$\mathcal{r}$ for $\mathbb{P}_{WiFi}(f)$	21.3	3.7	3.1	21.3	3.7	3.1
$\mathcal{r}$ for $\mathbb{P}_{LTE}(f)$	40.8	3.9	3.4	40.8	3.9	3.4
$c_{1,2,d,\aleph}/c_{1,1,d,\aleph}\vert_{dB}$	−1.5	−8.3	−15.2	−1.8	−8.3	−14.8
$c_{1,4,d,\aleph}/c_{1,2,d,\aleph}\vert_{dB}$	−1.3	−8.1	−14.1	−1.7	−8.5	−15.1
$c_{1,8,d,\aleph}/c_{1,4,d,\aleph}\vert_{dB}$	−1.3	−6.8	−14.0	−2.0	−8.3	−14.7
$c_{1,16,d,\aleph}/c_{1,8,d,\aleph}\vert_{dB}$	−0.9	−5.3	−10.0	−1.9	−8.1	−14.2
$c_{1,32,d,\aleph}/c_{1,16,d,\aleph}\vert_{dB}$	−0.	−5.1	−6.9	−1.7	−6.8	−13.5
$c_{1,64,d,\aleph}/c_{1,32,d,\aleph}\vert_{dB}$	−0.	−2.3	−0.7	−1.4	−5.3	−12.3
$c_{1,128,d,\aleph}/c_{1,64,d,\aleph}\vert_{dB}$	−0.	−1.0	−0.7	−0.7	−5.1	−7.3
$c_{1,256,d,\aleph}/c_{1,128,d,\aleph}\vert_{dB}$	−0.	−0.	−0.	−0.	−2.3	−5.6
$c_{1,512,d,\aleph}/c_{1,256,d,\aleph}\vert_{dB}$	−0.	−0.	−0.	−0.	−1.0	−2.6

TABLE IV
$\frac{c_{K,\mathcal{N},N,1}}{c_{1,N,1,1}}|_{\mathrm{dB}}$ WHEN $\vec{\wp}^{\mathcal{P}}_{k,\aleph} \equiv \vec{\wp}^{\mathcal{P},\mathrm{Ray}}_{\mathrm{REC},1}$, $\mathcal{N} = N$, AND $N_0 = 0$

Ntw.	$K/N_{\overline{ex}}$=	4	2	1	1/2	1/4	1/8	1/16	1/32
MTF_1 MTF_2	$\frac{c_{N_t,\mathcal{N},N,1}}{c_{1,N,1,1}}\vert_{dB}$ =	22	13	10	7	4	1	−2	−5
MTF_3	$\frac{c_{N_t,\mathcal{N},N,1}}{c_{1,N,1,1}}\vert_{dB}$ =	25	12	6	1	−3	−6	−9	−12

TABLE V
$\frac{c_{K,\mathcal{N},N,1}}{c_{1,N,1,1}}|_{\mathrm{dB}}$ WHEN $\vec{\wp}^{\mathcal{P}}_{k,\aleph} \equiv \vec{\wp}^{\mathcal{P},\mathrm{Ray}}_{\mathrm{REC},1}$, $\mathcal{N} = 2N$, AND $N_0 = 0$

Ntw.	$K/N_{\overline{\mathrm{ex}}}$=	4	2	1	1/2	1/4	1/8	1/16	1/32
MTF_1 MTF_2	$\frac{c_{N_t,\mathcal{N},N,1}}{c_{1,N,1,1}}\|_{dB}$ =	17	11	8	5	2	−1	−4	−7
MTF_3	$\frac{c_{N_t,\mathcal{N},N,1}}{c_{1,N,1,1}}\|_{dB}$ =	10	4	1	−2	−5	−8	−11	−14

$\vec{\wp}^{\mathcal{P},\mathrm{Ray}}_{\mathrm{REC},1}$ with $K = 1$ and $\mathcal{d} = 1$ from Tables II and III, whereas $c_{N_t,\mathcal{N},N,1}$ corresponds to $\vec{\wp}^{\mathcal{P},\mathrm{Ray}}_{\mathrm{REC},1}$ with $K \gg 1$, $N = \mathcal{N}$ and $\mathcal{d} = N$. Moreover, in Table IV, N must be ≥ 128 and the channel is selected as frequency-selective Rayeigh fading with $\mathcal{N} = N$ and $N_0 = 0$. From Table IV, one can see that by decreasing the ratio $K/N_{\overline{\mathrm{ex}}}$, it is possible to reduce $c_{N_t,\mathcal{N},N,1}/c_{1,N,1,1}$ and in turn reduce $\max_k\{\mathcal{p}_k\}$ in (21). This decrease is possible by increasing $N_{\overline{\mathrm{ex}}}$ when K is fixed.

Increasing $N_{\overline{\mathrm{ex}}}$: There are several ways to increase $N_{\overline{\mathrm{ex}}}$, which are as follows.

1) One way to increase $N_{\overline{\mathrm{ex}}}$ is by increasing $N_{\mathcal{J}}$ at Tx. Another advantage for increasing $N_{\mathcal{J}}$ for a fixed T_s when $\mathcal{d}|_{\mathrm{UL}} = N$, is to decrease $\max_k\{\mathcal{p}_k\}$ while increasing the *spreading gain* N [6], which is useful against unidentified or ignored interferers in both UL and DL. Increasing $N_{\mathcal{J}}$ at Tx in DL does not affect the desired capacity per MTF device $\mathcal{C}_{\mathfrak{d}}|_{\mathrm{DL}}$. It reduces the capacity per MTF device for the UL portion, without affecting the overall desired network capacity $\mathcal{C}_{\mathfrak{d}}|_{\mathrm{UL}}$.
2) Another way to increase $N_{\overline{\mathrm{ex}}}$ is by increasing $N_{\mathcal{J}}$ indirectly at Rx by taking advantage of the frequency-selective nature of a multipath-rich wireless channel, which forces N to be replaced by $\mathcal{N}$, or equivalently, forces $N_{\overline{\mathrm{ex}}}$ to be replaced by $\mathcal{N}_{\overline{\mathrm{ex}}} \triangleq \mathcal{N}(1 - \zeta_{\mathrm{ex}})$. This is often referred to as *multipath diversity*. In this case, $\vec{g}_{l,k}$ in (17) is replaced by $\vec{g}_{l,k,\mathrm{Ch}}$ in (18) at Rx. Another advantage for replacing $N_{\overline{\mathrm{ex}}}$ by $\mathcal{N}_{\overline{\mathrm{ex}}}$ is to increase $\mathfrak{L}_{\mathrm{dB}}$ by $(\mathcal{N}/N)_{\mathrm{dB}}$. The values of $c_{K,\mathcal{N},\mathcal{d},1}/c_{1,N,1,1}$ are shown in Table V when $\vec{\wp}^{\mathcal{P}}_{k,\aleph} \equiv \vec{\wp}^{\mathcal{P},\mathrm{Ray}}_{\mathrm{REC},1}$ $\forall k$, with $\mathcal{N} = 2N$ and $N_0 = 0$.

VI. RESULTS

In this section, we compile downlink and uplink results for the three MTF MA networks, MTF_1, MTF_2 and MTF_3, and compare them to current and future MA networks. All MTF results are obtained based on the theory established in Theorems III and IV, on the constraints and designs shown in Section IV, and on the assumptions selected in Section V [in particular (21) and (22) and Tables II–V]. In this section, all BL examples use $\mathcal{C}_{\mathrm{BL}}$ in (6) with $\mathcal{r}_{\mathrm{BL}} = 1.5$ when compliant with $\mathbb{P}_{\mathrm{WiFi}}(f)$ and $\mathcal{r}_{\mathrm{BL}} = 1.75$ when compliant with $\mathbb{P}_{LTE}(f)$.

A. Downlink Results

In order to compare the DL portions of MTF_1, MTF_2, and MTF_3 with current and future MA networks, we introduce the DL portions of a set of six BL MA networks $\{\mathrm{BL}_1, \mathrm{BL}_2, \mathrm{BL}_3, \mathrm{BL}_4, \mathrm{BL}_5, \mathrm{BL}_6\}$ with BL_1 to be compared with MTF_1, BL_2 to be compared with MTF_2, and $\{\mathrm{BL}_3, \mathrm{BL}_4, \mathrm{BL}_5, \mathrm{BL}_6\}$ to be compared with MTF_3. BL_1 and BL_2 use the same unlicensed bands, the same BW and offer the same capacities as MTF_1 and MTF_2, respectively, whereas the set $\{\mathrm{BL}_3, \mathrm{BL}_4, \mathrm{BL}_5, \mathrm{BL}_6\}$ uses mm-wave bands with a 3.5-GHz BW, in order to offer the same capacity as MTF_3. All examples use a 16 dBi gain antenna and a 30-dBm transmit power at Tx of the BS/AP. All MTF examples use Tables II and III with $\mathcal{d} = 1$, $\mathcal{N} = \mathcal{N}_0 = 2N$ and either $\vec{\wp}^{\mathcal{P}}_{k,\aleph} \equiv \vec{\wp}^{\mathcal{P},\mathrm{Ric}}_{\mathrm{REC},1}$ for a LOS channel or $\vec{\wp}^{\mathcal{P}}_{k,\aleph} \equiv \vec{\wp}^{\mathcal{P},\mathrm{Ray}}_{\mathrm{REC},1}$ for an NLOS channel.

TABLE VI
DL RANGE RESULTS (IN GREEN) FOR MTF SYSTEMS WHEN $\vec{\wp}^{\mathcal{P}}_{k,\aleph} \equiv \vec{\wp}^{\mathcal{P}}_{\mathrm{REC},1}$, $\mathcal{d} = 1$, $\mathcal{N} = \mathcal{N}_0 = 2N$ COMPARED TO BL SYSTEMS

Network	f_c in GHz	$\mathcal{C}_{\mathfrak{d}}\|_{DL}$ in $Gbps$	$\mathcal{W}_m$ in $Gbps$	$\Re\|_{DL}$ for LOS & $\mathbb{P}_{WiFi}(f)$	$\Re\|_{DL}$ for NLOS & $\mathbb{P}_{WiFi}(f)$	$\Re\|_{DL}$ for LOS & $\mathbb{P}_{LTE}(f)$	$\Re\|_{DL}$ for NLOS & $\mathbb{P}_{LTE}(f)$
MTF_1	2.45	0.2	0.02	$17.0Km$	$2.5Km$	$15.1Km$	$2.1Km$
BL_1	2.45	0.2	0.02	$677m$	$138m$	$285m$	$72m$
MTF_2	5.8	2	0.02	$2.9Km$	$432m$	$1.4Km$	$278m$
BL_2	5.8	2	0.02	$0m$	$0m$	$0m$	$0m$
MTF_3	3.5	14	0.02	$2.2Km$	$338m$	$1.3Km$	$223m$
BL_3	26	14	3.5	$110m$	$35m$	$77m$	$26m$
BL_4	28	14	3.5	$102m$	$33m$	$72m$	$25m$
BL_5	38	14	3.5	$75m$	$27m$	$53m$	$20m$
BL_6	60	14	3.5	$48m$	$19m$	$34m$	$14m$

Table VI compares the DL ranges $\Re|_{\mathrm{DL}}$ for all three MTF examples with their BL counterparts, across either an LOS or an NLOS wireless channel compliant with either $\mathbb{P}_{\mathrm{WiFi}}(f)$ or $\mathbb{P}_{LTE}(f)$. Based on Table VI, it is possible to see that MTF MA networks offer an order of magnitude improvement in DL range $\Re|_{\mathrm{DL}}$ (shown in green) compared to their BL counterparts.

B. Uplink Results

Once again, the UL portions of the set of six BL MA networks $\{\mathrm{BL}_1, \mathrm{BL}_2, \mathrm{BL}_3, \mathrm{BL}_4, \mathrm{BL}_5, \mathrm{BL}_6\}$ are compared with their MTF counterparts. All examples use a 20-dBm transmit power at Tx of the device and a 0-dBi gain antenna at both Tx and Rx. All MTF examples use Table V with $\frac{K}{\mathcal{N}_{\min\overline{\mathrm{ex}}}} = \frac{1}{2}$, $\mathcal{d} = N_{\min}$, $\mathcal{N} = \mathcal{N}_0 = 2N$, and either $\vec{\wp}^{\mathcal{P}}_{k,\aleph} \equiv \vec{\wp}^{\mathcal{P},\mathrm{Ric}}_{\mathrm{REC},1}$ for an LOS channel or $\vec{\wp}^{\mathcal{P}}_{k,\aleph} \equiv \vec{\wp}^{\mathcal{P},\mathrm{Ray}}_{\mathrm{REC},1}$ for an NLOS channel, where $\mathcal{N}_{\min\overline{\mathrm{ex}}} \triangleq \mathcal{N}_{\min}(1 - \zeta_{\mathrm{ex}})$ and $\mathcal{N}_{\min} = 2N_{\min}$. In this case, K is either equal to 213, 2133, and 6416 for MTF_1, MTF_2, and MTF_3, respectively, when $\mathbb{P}_{\mathrm{Mask}}(f) \equiv \mathbb{P}_{\mathrm{WiFi}}(f)$, or equal to 408, 4080, and 12 270 for MTF_1, MTF_2, and MTF_3, respectively, when $\mathbb{P}_{\mathrm{Mask}}(f) \equiv \mathbb{P}_{LTE}(f)$.

Table VII compares the UL ranges $\Re|_{\mathrm{UL}}$ for all three MTF examples with their BL counterparts, across either an LOS or an NLOS wireless channel compliant with either $\mathbb{P}_{\mathrm{WiFi}}(f)$ or $\mathbb{P}_{LTE}(f)$. Once again, based on Table VII, it is possible to see that MTF MA networks offer several orders of magnitude improvement in UL range $\Re|_{\mathrm{UL}}$ (shown in green) compared to their BL counterparts.

TABLE VII
UL RANGE RESULTS FOR MTF SYSTEMS WHEN $\bar{\wp}^{\mathcal{P}}_{k,\aleph} \equiv \bar{\wp}^{\mathcal{P}}_{\mathrm{REC},1}$, $\frac{K}{\mathcal{N}_{\min_{\mathrm{Ex}}}} = \frac{1}{2}$, $\mathcal{d} = N_{\min}$, $\mathcal{N} = \mathcal{N}_0 = 2N$ COMPARED TO BL SYSTEMS

Network	f_c in GHz	$\mathcal{C}_{\mathfrak{b}}\|_{UL}$ in $Gbps$	$\mathcal{W}_m$ in $Gbps$	$\Re\|_{UL}$ for LOS & $\mathbb{P}_{WiFi}(f)$	$\Re\|_{UL}$ for NLOS & $\mathbb{P}_{WiFi}(f)$	$\Re\|_{UL}$ for LOS & $\mathbb{P}_{LTE}(f)$	$\Re\|_{UL}$ for NLOS & $\mathbb{P}_{LTE}(f)$
MTF_1	2.45	0.2	0.02	$4.9Km$	$848m$	$8.7Km$	$1.1Km$
BL_1	2.45	0.2	0.02	$34m$	$14m$	$14m$	$8m$
MTF_2	5.8	2	0.02	$6.5Km$	$773m$	$3.0Km$	$442m$
BL_2	5.8	2	0.02	$0m$	$0m$	$0m$	$0m$
MTF_3	3.5	6	0.02	$10Km$	$1.1Km$	$8.1Km$	$910m$
BL_3	26	6	3.5	19m	$10m$	$17m$	$8m$
BL_4	28	6	3.5	18m	$9m$	$15m$	$8m$
BL_5	38	6	3.5	13m	$7m$	$11m$	$6m$
BL_6	60	6	3.5	9m	$5m$	$7m$	$4m$

VII. CONCLUSION

Current communication systems are inherently TL. This implies that, by definition, they must contain high-frequency components. When such systems are constrained by a spectral mask, their high-frequency components fall far below the noise floor, and traditionally ignored. This article shows that by taking advantage of such components it is possible to significantly improve the capacity of current communication systems, without having to modify their spectral footprint.

APPENDIX

A. Proof of Theorem I

According to [7, eq. (1.4)], when $\vec{\alpha}$ and $\vec{w}$ in (3) are independent and Gaussian, the input–output mutual information, $I(\vec{\alpha}, \vec{r}/\boldsymbol{h}_{\mathrm{Ch}})$ conditioned on $\boldsymbol{h}_{\mathrm{Ch}}$ of (3), is

$$I\left(\vec{\alpha}, \vec{r}/\boldsymbol{h}_{\mathrm{Ch}}\right) = \sum_{k=1}^{\mathrm{rank}(\boldsymbol{h}_{\mathrm{Ch}})} \log_2\left(1 + \Lambda_k \frac{\bar{\mathcal{A}} K \mathfrak{p}}{\mathbb{N}_o f_s}\right) \tag{A1}$$

where Λ_k is the kth-squared singular value of normalized $\boldsymbol{h}_{\mathrm{Ch}}$ and $\frac{\bar{\mathcal{A}} K \mathfrak{p}}{\mathbb{N}_o f_s}$ is the average transmitted SNR. Equation (A1) implies that

$$\mathcal{C}_{\mathrm{TL}} = \frac{1}{MT_s}\, I\left(\vec{\alpha}, \vec{r}/\boldsymbol{h}_{\mathrm{Ch}}\right). \tag{A2}$$

■

B. Proof of Theorem II

When $\Lambda_k \frac{\bar{\mathcal{A}} K \mathfrak{p}}{\mathbb{N}_o f_s} \ll 1$, $\mathcal{C}_{\mathrm{TL}} \approx \log_2 e \cdot \bar{\Lambda} \cdot \frac{\bar{\mathcal{A}} K \mathfrak{p}}{\mathbb{N}_o}$ where $\bar{\Lambda}$ is the arithmetic mean of Λ_k. As $\mathcal{M} \gg 1$, $\boldsymbol{h}_{\mathrm{Ch}} \boldsymbol{h}^{\dagger}_{\mathrm{Ch}}$ is either asymptotically block toeplitz if $\mathcal{d} < N$ with a solution for Λ_k according to Szego's theorem [15, Th. 6.5] or block diagonal with a solution for Λ_k according to [7, Th. 3.6]. As a worst case scenario, we select $\mathcal{d} = 1$ and derive a lower-bound on $\bar{\Lambda}$. According to Szegö's theorem in [15], as $\mathcal{M} \gg 1$, $\bar{\Lambda}$ is asymptotically proportional to $tr(\frac{1}{2\pi}\int_{-\pi}^{\pi} \boldsymbol{H}_{B\_\mathrm{Ch}}(\Omega)\boldsymbol{H}^{\dagger}_{B\_\mathrm{Ch}}(\Omega)d\Omega)$ where $\boldsymbol{H}_{B\_\mathrm{Ch}}(\Omega)$ is the DTFT of the first $\mathcal{M} \times K$ block of $\boldsymbol{h}_{\mathrm{Ch}}$.

Based on DOD Properties I and II, it is possible to express the kth column of $\boldsymbol{H}_{B\_\mathrm{Ch}}(\Omega)$ as

$$\sqrt{1/\Gamma_k} \sum_{l} \Theta_{l,k}\ (\Omega)\, (N\ \mathrm{diric}\,(\Omega, N))^{\aleph_{l,k}} \not{\boldsymbol{\phi}}_{l,k}\,(\Omega)$$

where $\Theta_{l,k}(\Omega)$ is a set of random processes (RP), $\mathrm{diric}(\Omega, N) \triangleq \frac{\sin(\frac{\Omega N}{2})}{N \sin(\frac{\Omega}{2})} \triangleq \frac{\mathrm{sinc}(\frac{\Omega N}{2\pi})}{\mathrm{sinc}(\frac{\Omega}{2\pi})}$ is the *Dirichlet* function (aliased sinc), $\not{\boldsymbol{\phi}}_{l,k}(\Omega)$ is a continuous-frequency function with $\mathrm{DOD} = 0$ and Γ_k is a normalization constant. As $N \gg 1$

$$tr\left(\frac{1}{2\pi}\int_{-\pi}^{\pi} \boldsymbol{H}_{B\_\mathrm{Ch}}\,(\Omega)\, \boldsymbol{H}^{\dagger}_{B\_\mathrm{Ch}}\,(\Omega)\, d\Omega\right) \to \sum_{k=1}^{K} \frac{2}{N\Gamma_k}$$

$$\times \int_{-\frac{N}{2}}^{\frac{N}{2}} \left|\sum_{l} \Theta_{l,k}\left(\frac{2\pi\Omega}{N}\right) N^{\aleph_{l,k}}\ \mathrm{sinc}^{\aleph_{l,k}}\,(\Omega)\, \not{\boldsymbol{\phi}}_{l,k}\left(\frac{2\pi\Omega}{N}\right)\right|^2 d\Omega.$$

As $N \gg 1$, $N^{\aleph_{l,k}}\ \mathrm{sinc}^{\aleph_{l,k}}(\Omega) \to \Omega^{-2\aleph}$ where $\min_{l,k}\{\aleph_{l,k}\} = \aleph$. Using Chebyshev's inequality, $\bar{\Lambda}$ is lower-bounded by a function $\propto \frac{1}{N}\int_{-\frac{N}{2}}^{\frac{N}{2}} \Omega^{-2\aleph} d\Omega$, which is $\propto N^{-2\aleph}$. This proves that doubling $\mathcal{C}_{\mathrm{TL}}$ in (A2) across its medium-SNR region requires increasing $\bar{\mathcal{A}} K \mathfrak{p}$ by a fixed multiple of $2^{2\aleph}$. ■

C. Proof of Theorem III

When $\vec{\alpha}$ in (1) is Gaussian, $\boldsymbol{h}_{\mathrm{Ch}}\,\vec{\alpha}$ is also Gaussian. In this case, $\boldsymbol{h}_{\mathrm{Ch}}\,\vec{\alpha}$ and $\vec{w}$ in (3) are independent and Gaussian, implying that the ith iteration at the MMSE-SIC detector at Rx is information-lossless in terms of the input–output mutual information [23]. According to [6, eq. (8.71)], we have

$$\mathcal{C}_{\mathrm{TL}} = \frac{1}{MT_s} \sum_{i=1}^{Q} \log_2\left(1 + \rho_{\mathrm{MMSE}_i}\right)$$

where at the ith iteration, ρ_{MMSE_i} is the MMSE at the output of the TL channel, defined as [7] $\mathrm{SNR}_i/\boldsymbol{\rho}_i$, with SNR_i the received SNR at the ith iteration and $\frac{1}{\boldsymbol{\rho}_i}$ its *multiuser efficiency*, corresponding to the ith column in $\boldsymbol{h}_{\mathrm{Ch}}$, assuming no error propagation in the previous iterations.

According to [7, eq. (1.8)], the arithmetic mean $\overline{\rho_{\mathrm{MMSE}_i}}$ of the MMSE at the ith iteration is equal to $\sum_{k=1}^{Q-i+1} \frac{1}{1+\Lambda_{k,i}\mathrm{SNR}_i}$ where $\Lambda_{k,i}$ is the kth-squared singular value of $\boldsymbol{h}_{\mathrm{Ch}^i}$ defined as the matrix $\boldsymbol{h}_{\mathrm{Ch}}$ obtained after removing all columns and all rows corresponding to previously detected symbols and after ordering the remaining columns of $\boldsymbol{h}_{\mathrm{Ch}}$ according to a nondescending MMSE value.

From Constraint 3, we have

$$\min_i \{\mathrm{SNR}_i/\boldsymbol{\rho}_i\} \triangleq \min_i \left\{\max_k \{\Lambda_{k,i}\}\, \mathrm{SNR}_i\right\} \geq 1.$$

As $N \gg 1$, $\boldsymbol{h}^{\dagger}_{\mathrm{Ch}^i}\boldsymbol{h}_{\mathrm{Ch}^i}$ is either asymptotically block Toeplitz or block diagonal. According to Szegö's theorem [12, Th. 6.5] as $N \gg 1$ the kth squared singular value $\Lambda_{k,i}$ is asymptotically

$\propto \frac{1}{2\pi}\int_{-\pi}^{\pi} \boldsymbol{H}^{\dagger}_{\mathrm{Ch}^{k,i}}(\Omega)\boldsymbol{H}_{\mathrm{Ch}^{k,i}}(\Omega)d\Omega$, where $\boldsymbol{H}_{\mathrm{Ch}^{k,i}}(\Omega)$ is the DTFT of N elements out of the $\mathcal{d}\times KN_{\mathcal{d}}$ *basic* block of $\boldsymbol{h}_{\mathrm{Ch}^{i}}$, sampled at the $\{k\text{th}, (k+K)\text{th}, \ldots, (k+(N_{\mathcal{d}}-1)K)\text{th}\}$ column. Similar to Appendix B, it is possible to express $\boldsymbol{H}_{\mathrm{Ch}^{k,i}}(\Omega)$ with $\mathrm{diric}(\Omega, N_{\mathcal{d}})$ replaced by $\mathrm{diric}(\frac{2\Omega}{N_{\mathcal{d}}}, N_{\mathcal{d}})$ s.t. $\lim_{N\to\infty}\mathrm{diric}(\frac{2\Omega}{N_{\mathcal{d}}}, N_{\mathcal{d}}) = \mathrm{sinc}(\Omega)$. Based on the aforementioned, as $N \gg 1$, the kth diagonal term $\Lambda_{i,k}$ in $\frac{1}{2\pi}\int_{-\pi}^{\pi} \boldsymbol{H}^{\dagger}_{\mathrm{Ch}^{k,i}}(\Omega)\boldsymbol{H}_{\mathrm{Ch}^{k,i}}(\Omega)d\Omega$ is lower-bounded by

$$\frac{1}{\Gamma_k}\frac{1}{\boldsymbol{r}}\frac{\mathcal{d}}{N}\int_{-\frac{N_{\mathcal{d}}}{2}}^{\frac{N_{\mathcal{d}}}{2}}\left|\sum_{l}\Theta_{l,k}\left(\frac{2\pi\Omega}{N_{\mathcal{d}}}\right)N_{\mathcal{d}}^{\aleph_{l,k}} \times \mathrm{sinc}^{\aleph_{l,k}}(\Omega)\,\not{\mathfrak{f}}_{l,k}\left(\frac{2\pi\Omega}{N_{\mathcal{d}}}\right)\right|^2 d\Omega.$$

As $N_{\mathcal{d}} \gg 1$, $N_{\mathcal{d}}^{\aleph_{l,k}}\ \mathrm{sinc}^{\aleph_{l,k}}(\Omega) \to \Omega^{-2\aleph}$ where $\min_{l,k}\{\aleph_{l,k}\} = \aleph$. Using Chebyshev's inequality, $\Lambda_{k,i}$ is lower-bounded by a function $\propto \frac{1}{\boldsymbol{r}}\frac{\mathcal{d}}{N}\int_{-\frac{N_{\mathcal{d}}}{2}}^{\frac{N_{\mathcal{d}}}{2}}\Omega^{-2\aleph}d\Omega$, which is $\propto \frac{1}{\boldsymbol{r}}N_{\mathcal{d}}^{-2\aleph}$. Now, we need to find $\min_i\{\max_k\{\Lambda_{k,i}\}\}$. Instead, we find its lower-bound $\min_k\{\Lambda_{k,i}\}$. Based on [24, eq. (17)], $\min_k\{\Lambda_{k,i}\}$ is $\propto \sum_{k=1}^{K} k^{-2\aleph}\frac{1}{\boldsymbol{r}}N_{\mathcal{d}}^{-2\aleph}$ as $N_{\mathcal{d}} \gg 1$. Based on Faulhaber's formula, $\sum_{k=1}^{K} k^{-2\aleph} \approx \frac{K^{1-2\aleph}}{1-2\aleph}$ and $\boldsymbol{\mathcal{p}}_i$ is upper-bounded by a function $\propto \frac{1}{\boldsymbol{r}}K^{2\aleph-1}N_{\mathcal{d}}^{2\aleph}$ as $N \gg 1$. ■

D. Proof of Theorem IV

Since $\{\boldsymbol{h}_{\mathrm{MTF}}\}_k \triangleq \vec{\wp}_{k,\aleph} + \vec{\wp}_{k,0}$ in (8), therefore, Constraints 1–3 imply that both the numerator of $\boldsymbol{\mathcal{p}}_k$ and its denominator consist of the sum of two terms, each corresponding to the terms, $\vec{\wp}_{k,\aleph}$ and $\vec{\wp}_{k,0}$, respectively. The numerator terms are $\mathfrak{p}$ and $\frac{N_0}{\mathcal{R}/\urcorner}$, respectively, whereas the denominator terms are $\mathfrak{p}/(\boldsymbol{c}_{K,N,\mathcal{d},\aleph}\ \frac{1}{\boldsymbol{r}}K^{2\aleph-1}N_{\mathcal{d}}^{2\aleph})$ and $\boldsymbol{c}_{N_0,0}\frac{\boldsymbol{r}N_0}{\mathcal{R}N/\urcorner}$, respectively. Thus

$$\boldsymbol{\mathcal{p}}_k \propto \frac{1 + \frac{N_0}{\lambda\mathcal{R}}}{\frac{1}{\boldsymbol{c}_{K,N,\mathcal{d},\aleph}\ \frac{1}{\boldsymbol{r}}\ K^{2\aleph-1}N_{\mathcal{d}}^{2\aleph}} + \boldsymbol{c}_{N_0,0}\ \frac{\boldsymbol{r}N_0}{\lambda\mathcal{R}N}}$$

where $\lambda \triangleq \mathfrak{p}/\urcorner$ according to Constraint 2. ■

REFERENCES

[1] A. D. Wyner, "The capacity of the band-limited Gaussian channel," *Bell Syst. Tech. J.*, vol. 45, no. 3, pp. 359–395, Mar. 1966.

[2] D. Gabor, "Theory of communication," *Proc. IEEE*, vol. 93, no. 26, pp. 429–457, Nov. 1946.

[3] R. S. Cheng and S. Verdu, "Capacity of root-mean-square band-limited Gaussian channels," *IEEE Trans. Inf. Theory*, vol. 37, no. 3, pp. 453–465, May 1991.

[4] T. J. Cruise, "Channel capacity for an RMS bandwidth constraint," MIT RLE, Cambridge, MA, USA, Quart. Prog. Rep. 90, Jul. 1968.

[5] D. Parsavand and M. K. Varanasi, "RMS bandwidth constrained signature waveforms that maximize the total capacity of PAM-synchronous CDMA channels," *IEEE Trans. Commun.*, vol. 44, no. 1, pp. 65–75, Jan. 1996.

[6] D. Tse and P. Viswanath, *Fundamental of Wireless Communication*. Cambridge, U.K.: Cambridge Univ. Press, 2005.

[7] A. M. Tulino and S. Verdu, *Random Matrix Theory and Wireless Communication*. Delft, The Netherlands: NOW Publishers Inc., 2004.

[8] R. G. Gallager, *Information Theory and Reliable Communication*. Hoboken, NJ, USA: Wiley, 1968.

[9] K. Barman and O. Dabeer, "Capacity of MIMO systems with asynchronous PAM," *IEEE Trans. Commun.*, vol. 57, no. 11, pp. 3366–3375, Nov. 2009.

[10] D. N. C. Tse and S. Verdu, "Optimum asymptotic multiuser efficiency of randomly spread CDMA," *IEEE Trans. Inf. Theory*, vol. 46, no. 7, pp. 2718–2722, Nov. 2000.

[11] M. A. Sedaghat, R. Müller, and F. Marvasti, "On optimum asymptotic multiuser efficiency of randomly spread CDMA," *IEEE Trans. Inf. Theory*, vol. 61, no. 12, pp. 6635–6642, Dec. 2015.

[12] A. Goldsmith, S. A. Jafar, N. Jindal, and S. Vishwanath, "Capacity limits of MIMO channels," *IEEE J. Sel. Areas Commun.*, vol. 21, no. 5, pp. 684–702, Jun. 2003.

[13] A. S. Y Poon, R. W. Brodersen, and D. N. C. Tse, "Degrees of freedom in multiple-antenna channels: A signal space approach," *IEEE Trans. Inf. Theory*, vol. IT-51, no. 2, pp. 523–536, Feb. 2005.

[14] D. Shiu, G. J. Foschini, M. J. Gans, and J. M. Kahn, "Fading correlation and its effects on the capacity of multielement antenna systems," *IEEE Trans. Commun.*, vol. 48, no. 3, pp. 502–513, Mar. 2000.

[15] J. Gutierrez-Gutierrez and P. M. Crespo, "Block Toeplitz matrices: Asymptotic results and applications," *Found. Trends Commun. Inf. Theory*, vol. 8, no. 3, pp. 179–257, Jan. 2011.

[16] The International Telecommunication Union, "Unwanted emissions in the out-of-band domain," Spectrum Management Series, Recommendation ITU-R SM.1541-4, Sep. 2011.

[17] A. I. Saichev and W. Woyczynski, *Distributions in the Physical and Engineering Sciences*, vol. 1. New York, NY, USA: Springer, 1996, sec. 3.2, p. 78.

[18] Z. Kadelburg *et al.*, "Inequalities of Karamata, Schur and Muirhead, and some applications," *Teaching Math.*, vol. VIII, no. 1, pp. 31–45, 2005.

[19] M. Lopez-Benitez *et al.*, "Spectral occupation measurements and blind standard recognition sensor for cognitive radio networks," in *Proc. 4th Int. Conf. Cogn. Radio Oriented Wireless Netw. Commun.*, 2009, pp. 1–9.

[20] F. H. Sanders, "Broadband spectrum surveys in Denver, CO, San Diego, CA, and Los Angeles, CA: Methodology, analysis, and comparative results," in *Proc. IEEE Int. Symp. Electromagn. Compat.*, Aug. 1998, vol. 2, pp. 988–993.

[21] M. A. McHenry *et al.*, "Spectrum occupancy measurements," Shared Spectrum Company, technical reports, Jan. 2004 to Aug. 2005. [Online]. Available: http://www.sharedspectrum.com/measurements

[22] A. Weil, *Number Theory: An Approach Through History*. New York, NY, USA: Springer-Verlag, 1983.

[23] D. Guo, S. Shamai, and S. Verdú, "Mutual information and MMSE in Gaussian channels," *IEEE Trans. Inf. Theory*, vol. IT-51, no. 4, pp. 1261–1282, Apr. 2005.

[24] H. Zhang, F. Niu, H. Yang, and D. Yang, "Polynomial PDF of the smallest eigenvalue of complex central Wishart matrix with correlation at the side with the smallest number of antennas," *IEEE Commun. Lett.*, vol. 12, no. 10, pp. 749–751, Dec. 2008.

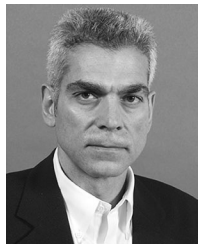

Michel Fattouche received the M.A.Sc. and Ph.D. degrees from the University of Toronto, Toronto, ON, Canada, in 1982 and in 1986 respectively.

He is currently is an Emeritus Professor with the Department of Electrical and Computer Engineering, Schulich School of Engineering, University of Calgary, Calgary, AB, Canada. His research work has led to 26 patents issued and 17 pending. Based on his research in wideband orthogonal frequency division multiplexing (W-OFDM), he cofounded Wi-LAN, Inc., in 1993, which led the IEEE to incorporate Wi-LAN's patented W-OFDM technology in its "WirelessMAN" Standard 802.16a. Based on his research on superresolution, he also cofounded Cell-Loc, Inc., in 1995, a developer of a family of network-based wireless location products with several networks deployed in Canada and in Brazil. More than 200 companies worldwide have licensed his patents.

Prof. Fattouche was named "Prairies Entrepreneur of the Year" in 2000 as part of the Ernst and Young's Entrepreneur of the Year Program.